

---

Masters Theses

Student Theses and Dissertations


---

Spring 2016

## Multifunctional wearable epidermal device for physiological signal monitoring in sleep study

J V M S Avinash Kankipati

Follow this and additional works at: [https://scholarsmine.mst.edu/masters\\_theses](https://scholarsmine.mst.edu/masters_theses)

 Part of the [Biomedical Commons](#), and the [Mechanical Engineering Commons](#)

Department:

---

### Recommended Citation

Kankipati, J V M S Avinash, "Multifunctional wearable epidermal device for physiological signal monitoring in sleep study" (2016). *Masters Theses*. 7739.  
[https://scholarsmine.mst.edu/masters\\_theses/7739](https://scholarsmine.mst.edu/masters_theses/7739)

This thesis is brought to you by Scholars' Mine, a service of the Missouri S&T Library and Learning Resources. This work is protected by U. S. Copyright Law. Unauthorized use including reproduction for redistribution requires the permission of the copyright holder. For more information, please contact [scholarsmine@mst.edu](mailto:scholarsmine@mst.edu).

MULTIFUNCTIONAL WEARABLE EPIDERMAL DEVICE FOR  
PHYSIOLOGICAL SIGNAL MONITORING IN SLEEP STUDY

by

J V M S Avinash Kankipati

A THESIS

Presented to the Faculty of the Graduate School of the  
MISSOURI UNIVERSITY OF SCIENCE AND TECHNOLOGY

In Partial Fulfillment of the Requirements of the Degree

MASTER OF SCIENCE

in

MECHANICAL ENGINEERING

2016

Approved by:

Dr. Xian Huang, Advisor

Dr. Frank Liou

Dr. Heng Pan

© 2016

J V M S Avinash Kankipati

All Rights Reserved

## ABSTRACT

Sleep is the essential part of life. Thousands of people are suffering from different kinds sleep disorders. Clinical diagnosing and treating for such disorders are costly, painful and quite sluggish. To reach the demand many commercial products are into the market to encourage home based sleep studies using portable devices. These portable devices are limited in use, cannot be handled easily and quite costly. Advancements in technology miniaturized these portable devices to wearable devices to make them convenient and economical. Elastic, soft and thin silicon membrane with physical properties well matched with that of the epidermis provides conformal and robust contact with the skin. Integration of an elastic and flexible electronics to such a membrane provides an epidermal electronic system (EES) that can enhance the robustness in operation for electrophysiological signal measurement. Biocompatible and non-invasive over the skin are the advantages of this class of technology that lie beyond those available with conventional, point-contact electrode interfaces to the skin. Recording of various long-term physiological signals relevant in various sleep studies can be performed using this multifunctional device. Optimized design of EES for monitoring various physiological signals like surface electroencephalography (EEG), electrooculography (EOG) and electromyography (EMG) are presented in this project.

## ACKNOWLEDGEMENTS

I would like to express my deep gratitude and sincere thanks to my advisor, Dr. Xian Huang for his guidance and support during this project. It was privilege for working on such an innovative and interesting project under Dr. Xian Huang.

I would also thank Dr. Frank Liou and Dr. Heng Pan for serving as my advisory committee.

I would thank Mechanical Department and Material Science Research Center of Missouri University of Science and Technology for allowing me to use their facilities for my research.

I would thank National Science Foundation (NSF) for funding my research.

I would also thank my fellow researcher Bikram Kishore Mahajan for guiding me throughout the research. I would like to thank Xiaowei Yu for her kind assistance for helping me in the fabrication for the research.

I would thank Abishek Kodi, Sujith Anumolu and all my friends who supported me personally.

Lastly, I would like to thank my parents and family, for the immeasurable care, support and love they always have.

## TABLE OF CONTENTS

	Page
ABSTRACT.....	iii
ACKNOWLEDGEMENTS.....	iv
LIST OF ILLUSTRATIONS.....	vii
LIST OF TABLES.....	ix
 SECTION	
1. BACKGROUND .....	1
1.1. INTRODUCTION TO SLEEP .....	1
1.1.1. Paradigm of Sleep.....	3
1.1.2. Sleep Cycle.....	4
1.2. SLEEP DISORDERS .....	7
1.3. SLEEP CENTERS.....	9
1.3.1. Electrode Preparation and Methodology.....	11
1.3.2. Bio-physiological Signal Monitoring over the Skin.....	12
1.3.2.1. EEG .....	12
1.3.2.2. EOG.....	16
1.3.2.3. EMG.....	16
1.4. PORTABLE DEVICES FOR HEALTHCARE.....	18
1.5. ART OF WEARABLE DEVICES .....	20
1.6. NOVEL DEVICE FOR EPIDERMAL INTEGRATION.....	23
2. DESIGN AND FABRICATION .....	26

2.1. DESIGN OF THE SENSOR.....	26
2.2. SILICONE MEMBRANE FOR THE SENSOR .....	29
2.3. FABRICATION TECHNIQUES .....	32
3. EXPERIMENTAL SETUP & METHODS .....	38
3.1. PARAMETERS REQUIRED FOR SILICONE MEMBRANE TO MOUNT ON THE SKIN.....	38
3.1.1. Background. ....	39
3.1.2. Experimental Setup.. ....	42
3.2. EXTERNAL SIGNAL CONDITIONING CIRCUIT FOR MEASURING THE EPIDERMAL DEVICE.....	46
3.2.1. Setup for the In-Vivo Characterization of the EP Sensor.	53
3.2.2. Experimental Setup In-Vitro Characterization of the Strain Sensors.....	54
4. RESULTS.....	57
4.1. PEEL TEST .....	57
4.2. RESPONSE OF THE EP SENSORS FROM THE IN-VIVO TEST.....	59
4.3. RESPONSE OF THE STRAIN SENSORS FROM THE IN-VITRO TEST.....	63
5. SUMMARY AND CONCLUSIONS.....	65
6. ACKNOWLEDGEMENT .....	66
REFERENCES .....	67
VITA.....	72

## LIST OF ILLUSTRATIONS

	Page
Fig.1.1. Position of electrodes for polysomnography.....	5
Fig.1.2. International 10-20 system (A) Left (B) Right (C) Location and Nomenclature of intermediate 10% electrodes as per standards of American Electroencephalographic society.....	15
Fig.1.3. Block Diagram of a Typical Wearable Device.....	21
Fig.1.4. Side View of Layers of Human Skin.....	24
Fig.2.1. Functional parts of the epidermal sensor.....	26
Fig.2.2. EP sensor when observed under an SEM at (200 $\mu$ m).....	27
Fig.2.3. Graphite strips on the EES under an SEM (500 $\mu$ m).....	28
Fig.2.4. Exploded view of the schematic diagram of the sensor.....	28
Fig.2.5. Exploded view schematic diagram of the silicon membrane for the sensor.....	32
Fig.2.6. (a) to (n) Schematic illustration of steps for fabricating epidermal sensor. (o) to (r) Epidermal sensor mounted on the silicon membrane.....	33
Fig.2.7. Schematic exploded view of all the layers of the device.....	35
Fig.2.8. Transfer printing of device from glass slide to water-soluble film.....	36
Fig.2.9. Flexibility of the device on the silicone membrane.....	36
Fig.2.10. Twisting of the device on the silicone membrane.....	37
Fig.3.1. Layers of Silicone Membrane.....	38
Fig.3.2. Elastic film peeling from a rigid substrate.....	40
Fig.3.3. Mark-10 Force Gauge.....	43
Fig.3.4. Schematic representation of layers of silicon membrane during the peel test for measuring the peel force between the silicone layer and backing layer.....	44
Fig.3.5. Backing layer being peeled from the silicone membrane on the tensile tester....	45



Fig.3.6. Schematic representation of layers of silicon membrane during the peel test for measuring the peel force between the adhesive layer and skin. ....	45
Fig.3.7. Peeling of the adhesive layer from the skin by the tensile tester.....	46
Fig.3.8. Nomenclature of various pads of the epidermal sensor.....	47
Fig.3.9. External Bluetooth Circuit.....	48
Fig.3.10. External conditioning circuit for the epidermal sensor to measure the graphite resistance.....	51
Fig.3.11. Setup for capturing the EP Signals .....	53
Fig.3.12. Device fixed on a stretcher .....	54
Fig.3.13. Experimental setup for measuring the change in the resistivity of the graphite strips due to mechanical strain.....	55
Fig.3.14. Nomenclature of the directions based on graphite strips.....	56
Fig.4.1. Force between Acetate film and Silicone .....	57
Fig.4.2. Force between Silicone Adhesive and Skin .....	58
Fig.4.3. Force vs Time for Acetate Film and Silicone.....	59
Fig.4.4. Sensor location on the scalp for EEG measurement.....	60
Fig.4.5. Plot of EEG signals obtained as per the position shown in Fig 4.4.....	60
Fig.4.6. Sensor location on the scalp for EOG measurement .....	61
Fig.4.7. Plot of EOG signals obtained as per the position shown in Fig. 4.6. ....	61
Fig.4.8. Sensor location on the scalp for EMG measurement .....	62
Fig.4.9. Plot of EOG signals obtained as per the position shown in Fig 4.8. ....	62
Fig.4.10. Percentage Change in resistance of the graphite strips when expanded in direction 1 .....	63
Fig.4.11. Percentage Change in resistance of the graphite strips when expanded in direction 2 .....	64

**LIST OF TABLES**

	Page
Table.2.1. Maximum force required to peel the backing layer (3M Scotchpak TM Release Liner Fluoropolymer Coated Polyester Film, 3M, USA) with different lubricants as buffer.....	31
Table.2.2. Maximum force required to peel the acetate film from various types of silicon membranes. ....	31
Table.3.1. BITalino specifications .....	48
Table.3.2. Nomenclature of the pads and their mode of measurement.....	49
Table.3.3. Range of spectrum to set the filters for different EP signals [49] [37] [54]. ...	52
Table.4.1. Gauge factor of the graphite strips in direction1 & 2 .....	64

# 1. BACKGROUND

## 1.1. INTRODUCTION TO SLEEP

Humans contribute one third of their life to sleep. Sleep is the most essential thing required for the human body. It involves naturally repetitive state of the brain characterized by altered consciousness, relatively inhibited activity in the reflexes and almost all voluntary muscles.

Reduced ability to respond to the stimuli differentiates wakefulness from sleep. Discontinuous period of hibernation or in a state of comatose are different from sleep. The internal circadian clock regulates the biological clock of the human body in the functioning of wakefulness and sleep. Sleep is essential in order to build skeletal, muscular, nervous and immune systems.

Almost all living things in the world have rest in the form sleep in one form or the other. Lack of sleep may leads to many chronic diseases related to both physical and mental health. The disorders originated due to improper sleep are sleep-disordered breathing, restless legs syndrome, insomnia, narcolepsy, sleep apnea, sleep-related neurological disorders, sleep-related medical disorders, and circadian rhythm sleep disorders. The consequences of sleep loss were obesity, diabetes, heart disease, hypertension, mood disorders, improper immune functioning and many more. In order to treat these types of diseases, proper understanding is necessary on the basic paradigm of normal sleep. Abnormal sleep is differentiated based on the standard sleep structure.

Sleep in mammal's acts in recurring periods, which involves body changes between two different categories Non-Rapid Eye Movement (NREM) and Rapid Eye Movement

(REM) sleep. Depending on the type of brain wave activity, eye movements and muscle tone they have been categorized as 4 NREM and 1 REM sleep. The sleep patterns may vary extensively among animals and human beings.

In humans, chronological changes influence the sleep pattern. The age sleep architecture changes continuously and considerably with age. The percentage of sleep spent in various stages of the sleep changes from infancy to adulthood. Human development and successful aging was more conspicuous by sleep characteristics by age and their functions. For newborns and infants at birth, the circadian rhythms are not fully developed. The sleep starts with REM, progresses with one or two sleep cycles during the entire sleep. As the child grows older, amount of sleep decreases. During the adolescent age, puberty places an important role in sleep rather than study of sleep based on chronological age. The REM sleep and total sleep period decreases with increase in age.

Sleep patterns vary even with the genders. Differences found to be eminent in adults. Usually women maintain more SWS period than men do. Menstrual cycle influence the sleep-wake activity in the females. Sleep latency is more and ability to maintain the sleep was more difficult in the older people. Decline in sleep efficiency and quality are considered to be healthy for the older adults. Older people experience decrease in melatonin levels, which affect the gradual deterioration of circadian rhythms.

During sleep, there are many changes in the body system. Some of the physiological changes observed during the sleep in the systems are as follows [1]. According to the conservation of energy, sleep helps in storing some energy. Deprivation in the sleep leads to increase in energy consumption. Restoration of tissues and growth was the essential activity during sleep. Cell mitosis, protein synthesis and sleep growth hormone excretion

are high in the initial stages of sleep. During the growth, the NREM sleep was increased in a normal sleep cycle. Disturbance in the emotional behavior was due to sleep deprivation. NREM sleep is responsible for regulation of emotions, for instance deprivation of SWS induces hypochondriacally or depressive states. REM sleep plays a crucial role in neural maturation. In accordance with that percentage of REM sleep decreases with the age of the human being (children spend 80% of sleep in REM while adult people have 25% of REM sleep). Both NREM and REM sleep play an important role in memory and learning. During sleep, the information is transferred between cortex and hippocampus that realizes the fixation of memory traces. Learning is done due to the reprocessing of information in the brain. This chapter provides an overview on architecture of normal sleep cycle.

There are many significant changes in the body during various stages of sleep some of them are as follows.

- During sleep there are some changes in blood pressure and heart rate and can be observed in the autonomic nervous systems. Awakening leads to sharp increase in heart rate and blood pressure.
- When an individual is in deep NREM sleep, there will be a decrease in the sympathetic-nerve activity. REM sleep has more sympathetic-nerve activity compared to wakefulness.
- During REM sleep ventilation and respiratory flow becomes more erratic and increasing as compared to NREM sleep.

**1.1.1. Paradigm of Sleep.** Sleep Paradigm refers to simple structural orientation of normal sleep. As discussed earlier there are two types of sleep, NREM and REM sleep. REM can be distinguished from NREM by observing downsize in the physiological

activity in the eye movement and electrical activity of the brain waves. The sleep is generally divided into five stages that consist one cycle of sleep. Within these five stages, each stage has unique characteristics. The first four stages constitute to NREM sleep followed by REM sleep. In general, sleep of a person consists of 4 to 5 sleep cycles. There are several parameters involved in the characteristics such as muscle tone, brain wave movements and eye movements. As sleep gets immense, a slight decrease of breath rate as well as heart pace, EEG activity of the brain waves shifts to higher amplitude and the readings gets slower and blood pressure drops.

Many sleep diagnostic tests as sleep latency test, polysomnography, sleep apnea test and many more are been adopted by the clinics to monitor the sleep of an individual. It generally consists of recording the brain activity, eye movement and muscle movement which are done by electroencephalogram (EEG), electrooculogram (EOG) and electromyogram (EMG) respectively. The position of the electrodes in order to record the EOG, EEG and EMG measurement on a human face as shown in Fig 1.1. The details of the EOG, EEG and EMG will be discussed detail in the later sections of this chapter. The data obtained was recorded on the basis of an epoch.

**1.1.2. Sleep Cycle.** The sleep cycle constitutes to NREM and REM sleep in five stages where the 4 stages of NREM sleep ranging from light to deep sleep from stage 1 to 4. This section provides an overview of these states of sleep. Sleep generally starts with a small period of NREM stage 1 proceeds to stage 2, followed by stages 3 followed by stage 4 and finally enters into REM sleep. After the person enters to REM sleep he progresses to NREM of next sleep cycle. Approximately three fourth period of entire sleep will be spent in NREM and remaining period in REM sleep. The mean time of first cycle of sleep is

around 70 to 100 minutes and the later cycles last for a longer duration of approximately 90 to 120 minutes [2].

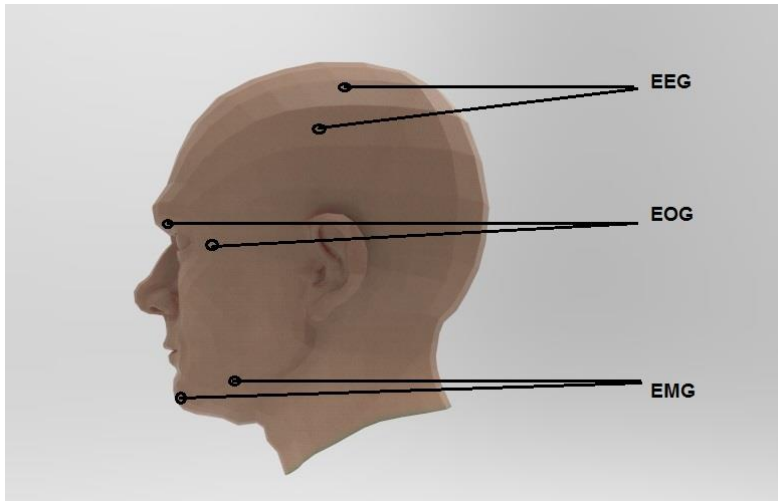


**Fig.1.1.** Position of electrodes for polysomnography

The NREM sleep classified into four different stages based on the physiology in body moments and distinct brain activity i.e. from lightest to the deep sleep. The parameters involved in sleep stages during a sleep cycle according to a normal healthy human being are as follows [1] [2].

Epilepsy differentiates normal sleep based on the EEG signal by the alpha, beta, delta and theta waves. The most important parameter to differentiate between wakefulness and sleep according to EEG was waking measures EEG at low voltage of 10-30  $\mu\text{V}$  and mixed frequency (High tonic EMG and alpha activity in EEG). During the measure of EEG

in the pre-sleep period, movement time is a major variable to be considered whether the individual is awake.

The beginning stage of sleep in which it starts with NREM sleep constitutes to 2 to 5 percent of sleep cycle. Sleep can be disturbed with noise or any external parameters in this stage. EEG measurements during this phase have low voltage rhythmic alpha waves with sharp vertex and mixed frequency waves <sup>[1][2]</sup>. Stage 1 is completed when the alpha activity amalgamates with EEG mixed frequency (alpha activity < 50% epoch) [1]. The gain in amplitude of chin EMG, the amplitude lowers from wakefulness to sleep and even a decrease can be observed from stages 1 to 3.

Stage 2 sleep of NREM sleep contributes to 45 to 55 percent of entire sleep period. The duration tends to increase with successive cycle. In order to be awake at this stage, the individual needs more intense stimuli than that of stage 1. Sleep spindles and K-complexes with mixed frequency activity and low voltage are observed in the EEG activity of the brain in this phase. Absence of slow waves, K complex is the sharp negative wave progressed by a little positive wave. Stage 2 can be scored if there any two succeeding occurrences of K complexes or sleep spindles less than 3 min.

Third NREM sleep stage and the next stage are considered as slow-wave sleep (SWS).It constitutes to 3 to 8 percent of sleep and last for a few minutes. Slow wave activity and increased high voltage are observed in EEG. Scoring stage 3 if 20-50 % epoch waves with 2 Hz or slower with amplitudes of 75  $\mu$ V. Typically, in stage 2 and 3 EMG activity is ignored. The downfall of EMG amplitude during the REM sleep reflects the normalized skeletal-muscle hypotonia corresponding to that particular sleep stage.



Stage four covers about 10 to 15 percent of sleep and referred as SWS. The brain activity from the EEG can be characterized by increase in high voltage as well as slow wave activity. When 50 of 2 Hz and slower amplitude waves are observed for more than 50% of epoch stage 4 is scored.

In the fifth stage of sleep, the NREM sleep moves to REM sleep which is specified by desynchronized brain wave activity and rapid eye movements. This stage was portrayed by theta activity, saw tooth waveforms, and slow alpha activity with no arousal. The amplitude obtained during the REM sleep is either less than or equal to the minimum amplitude obtained during the NREM sleep. A drop in amplitude can be observed during the REM sleep if the gain in NREM sleep adjusts to higher amplitude. In the first cycle this stage lasts for 1 to 5 minutes and continues to prolong in the following sleep cycles. Dreams in sleep occur during this stage. EMG activity is very low during this stage. REM stage is scored when two sleep spindles or K complexes is less than 3 minutes. In a healthy adult body REM sleep period tend to increase as the sleep progresses and may contribute to major of the last one-third of the sleep period. Sometimes the stage 2 of NREM sleep continues in a way that stage 3 and 4 will be observed [2]. During the REM stage a relatively reduced chin EMG, low voltage and a mixed frequency EEG are observed conventionally.

## **1.2. SLEEP DISORDERS**

Multifarious sleep disorders like insomnia, obstructive sleep apnea, narcolepsy, snoring, sleep walking and many more chronic sleep diseases are prevailing and

proliferating in today's world [8-15]. Abnormal sleep patterns may be found in the depressed patients or patients who are suffering from sleep disorders.

Sleep disorders are classified as behavioral or environmental, psychiatric, respiratory-related, neurological, circadian-rhythm, developmental or neuropsychiatric and other sleep related sleep disorders. Diagnosing sleep disorders are diagnosed by one or more tests like nocturnal polysomnography (NPSG), continuous positive airway pressure (CPAP titration), split study, bi-level titration, REM behavior disorder (RBD), NPSG with end tidal CO<sub>2</sub>, multiple sleep latency test (MSLT), maintenance of wakefulness test (MWT), etc. Most of them involve measuring the EEG, EOG, ECG, EMG, respiratory flow, etc. For the current purpose, this project focuses on abnormalities in EEG, EOG and EMG signals in people suffering from sleep disorders like narcolepsy, sleeping sickness, restless leg syndrome, periodic limb movement disorder and as a part of diagnosis for different sleep tests [16].

Qualitatively or quantitatively it is hard to measure the depression. For instance a study was conducted by Diaz-Guerrero [17] the EEG recordings of depressed and manic-depressive psychotics had low voltage during light sleep, less number of sleep spindles and more changes during the deep sleep. Another set of study was conducted by Oswald [18] on patients suffering from the same disorder and found that the patients were more awake, longer sleep latency & less stage 4 deep sleep.

There is no stage 3 and reduced amount of REM sleep for patients suffering from obstructive sleep apnea (OSA). Long sleep latency and increased wake after sleep onset (WASO) are observed in the patients suffering from chronic insomnia. Stage 3 and REM sleep is also found to be reduced for chronic insomnia patients. People suffering with sleep

apnea, depression and narcolepsy have short REM latency. Increased REM latency is also observed for those who are sleeping in the unfamiliar or uncomfortable environment or anything that obstacles the quality of sleep [16].

### **1.3. SLEEP CENTERS**

Around 40 million people in U.S are suffering with various kinds of sleep disorders. According to WHO there are around 3000 types of sleep disorders. Diagnosis of most sleep disorders based on pattern recognition of clinical characteristics determined from the comprehensive sleep history and a physical examination. According to various surveys, the demand and budget for the sleep disorder clinics and sleep centers are rising every year because of the rapid increasing of the number of patients suffering from sleep disorders to the limited number of beds in the sleep centers and physicians available to monitor them. This large variation created the situation, that the patient needs a 2 week prior reservation in order to have his diagnosis in the sleep centers [1-2].

Traditionally sleep monitoring was done using ink-writing pens to produce the polygraph recording that are traced on a paper. The standard procedure to record the data in real time is through epochs i.e. the sleeping time is generally divided into epochs which corresponds to the length of each paper. The recording speed for a 30-cm page (30 s) is varied for the test [5]. In modern days the test is performed digitally, even then the 30-s epoch is the wanted window for scoring the sleep. The epoch is named based on the major contribution of that stage present during that epoch if there is on shift during an epoch. Movement time (MT) is scored if more than one-half of an epoch is obscured because of

the artifacts. Some sleep centers consider MT as wake. A score of 10 or more indicates that the patient is considered sleepy.

The data of the individual suffering from any such sleep disorders are monitored for few days. They are diagnosed based on the standard normal sleep pattern of a healthy individual. Then the appropriate drugs are given based on their diagnosis and then the patient is again monitored after giving the drug whether he is responding properly to the drug until his sleep patterns become normal.

Even the people taking the medication usually have a different pattern of sleep. For instance, an increased REM latency is observed for the people taking REM suppressants. The effect of drugs on depressed patients also has different polysomnography recordings. In particular effect of hepta-barbital (400 mg doses given during alternate nights) on depressed patients was monitored by EEG & EOG. Excessive wakefulness was distributed throughout the nights and during the deep sleep there was a slight increase in the frequency shifts [4]. After the therapy there was a decrease in all the differences of the recordings towards the normal sleep. These changes are more significant from the sleep of a healthy individual.

Common terms used during a regular sleep study. The total bed time is named as total recording time (TRT). The movement the lights are turned off (start of recording) is counted and when the lights are turned ON (termination of recording). Total sleep time (TST) is aggregate of amount of time spend in sleep stages 1,2,3,4, REM and MT. Duration between initial sleep and final awakening is the sleep period time (SPT). Wake time is named as wake after sleep onset (WASO). SPT comprises of TST and WASO before the final awakening. Sleep latency is time between start time of sleep monitoring and first

epoch of sleep while REM latency is the time between the first epoch of sleep and the first REM sleep. The total number of minutes is noted in order to know the proportion of time spent in various sleep stages. Sleep stages are either characterized based on percentage of TST (Stages 1-4 & REM) or SPT (Stages 1-4 and WASO).

**1.3.1. Electrode Preparation and Methodology.** Bio-potential (EEG, EOG &EOG are mainly focused in this project) of the patients are collected to the recording circuit using the electrodes. These recordings should have maximum waveform amplitude and free from the artifacts. As skin has many layers and it disturbs the conductance of these signals because of the skin impedance, epidermal layer of the skin is scrapped without disturbing the dermis (safe places of the body) in order to place the electrodes. Skin is scrubbed only on the areas where electrodes are placed in order to minimize the discomfort of the patient and to obtain the maximum waveform from the person. For obtaining optimum signal quality, all the input electrodes are selected in a manner that all of them have a similar impedance (close to one another) in order to avoid the artifact due to the impedance mismatch. The standard for electrode impedance upper limit for EEG& EOG is  $5k\Omega$  and  $10k\Omega$  for EMG.

To have the minimal impedance the skin is abraded around the area where electrodes are placed. Electrodes are considered in a manner that they have the ample length for imputing the electrode site to the head box.

There are two methods to affix the disk electrodes. Firstly electrolyte or electrode paste are used to fill the electrode discs. For fixing the electrode disc, flexible gauge squares are placed over them by compressed air in the collodion method.

The electrode paste is carefully placed over the electrode site in order to secure the electrodes over the scalp. Electrode discs over the remaining areas are fixed using a tape or a medical adhesive. After the tests the reusable electrode discs and wires are secured and will be cleaned and disinfected with proper protocols for the future use.

**1.3.2. Bio-physiological Signal Monitoring over the Skin.** Bio signals are derived on the basis of observing the electrophysiological, biomechanical or chemical process of a living thing from the extent of protein to sequence of the genes, neural or cardiac rhythms, to tissue to organs.

Bioelectric potentials are generated by various body parts such as nervous, muscular or glandular tissue also named as Biopotentials. They are generated due to the electrochemical activity of excitable cells (certain group of cells in the body) that conduct along the sensory and motor nervous system, muscle contraction, brain activity, eye movements, etc. This project mainly focuses on Biopotentials of EEG, EOG and EMG.

**1.3.2.1. EEG.** The spontaneous activity obtained from the brain or the scalp is the electroencephalography (EEG). The amplitude read by any device depends on the position and placement of the electrodes over the particular part of the body. For instance, the amplitude of EEG measured from brain and scalp are 100  $\mu$ V and 1-2 mV respectively with a signal bandwidth ranging from 1 to 50 Hz.

Two other activities namely evoked potential and single-neuron behavior are in general read with the EEG data. Evoked potentials are due to the responses of the stimulus which are usually below the noise level. Signal to noise ratio can be determined using the evoked signal for obtaining a proper EEG signal.

The study of the single neuron which are monitored using the micro electrodes, placed at particular cell that can be monitored, which helps in building a cell network that can signify the real attributes of the tissue. Central nervous system consists of many neural tissues which can drive many mechanisms within individual neurons or interaction between neurons during this manner the neurons will generate oscillatory activity named as neural oscillation. These oscillations can be either observed in the neurons as oscillations in membrane potential or action potentials which generate rhythmic patterns which produces oscillatory action of post synaptic neurons. When a group of neurons and their feedback connections tend to do a single task they produce oscillations, these macroscopic oscillations can be detected in EEG. Synchronization of firing patterns of neurons is obtained by the oscillatory activity of class of neurons and their feedback connections. The firing frequency obtained during the interaction of neurons is different from the frequency of individual neuron. The EEG can be studied by the different type of waves produced in the process namely alpha ( $\alpha$ ), beta ( $\beta$ ), theta ( $\theta$ ) and delta ( $\delta$ ) [6].

Alpha waves are detected in awoken person who close his eyes which are obtained from the occipital region with a frequency of 8 to 13 Hz of spectral frequency. Beta waves are arised from the parietal and frontal lobes with a frequency range of 13 to 30 Hz.

Delta Waves are high amplitude brain waves possessing a frequency of 0 to 4 Hz. The range of waves are generally observed from EEG of an individual during his deep stage 3 of NREM sleep also known as slow-wave-sleep (SWS). Typically such waves describe the depth of the sleep. The waves tend to appear in deep sleep within stage 3 at less than 50% and appear more in the stage 4. Frequency band of theta waves are 4-8 Hz.

Brain activity on an EEG shows relatively low-voltage, mixed-frequency activity characterized by the presence of sleep spindles and K-complexes and above characterized waves across various stages of an individual's sleep. Sleep spindles are important for memory consolidation. Sleep Spindles are oscillatory waves from the brain activity in the stage 2 sleep. They have a characteristics of 12-14 Hz waves that reproduce for every 0.5 sec.

K complexes are observed during the stage 2 NREM sleep which usually signifies two functions, one of them is the response of the cortical arousal to the stimulus is very low and supporting memories during the sleep. In general K complex shows a voltage greater than 100  $\mu\text{V}$  and can be observed transiently with a high voltage peak (negative) proceeded by slow positive complex followed by the sleep spindles. K complexes are in general response to the external stimuli and are about 0.8Hz during the stage 2 sleep.

The level of consciousness reflects the EEG signal. The alpha waves are dominated in the EEG when the eyes were closed, when the person enters sleep the frequency of the EEG decreases. During the REM sleep the EEG has a definite pattern while the person enters to deep sleep EEG can be seen in delta waves with large and slow deflections.

The electrodes are placed based on the scalp based on *International 10-20 system of electrode placement* [6]. In this procedure 21 electrodes were placed on the scalp for measuring the EEG signal as shown in Fig 1.2.

Nasion and inoin are the reference points on the head. The skull perimeters are measured in the transverse and median planes based on these points. These perimeters are divided into 10% and 20% intervals for determining the electrode positions. In addition to them 3 other electrodes are placed as shown in Fig 1.2. b.



In addition to 21 electrodes additional 10% intermediate electrode positions are also used. The locations and nomenclatures are designed as per the American Electroencephalographic Society.

For measuring the EEG as per American Electroencephalographic Society standards a single central channel referenced to an ear mastoid site ( $C_4-A_1$ ), a single frontal channel referenced to an ear mastoid site ( $F_4-A_1$ ) and a single occipital channel referenced an ear mastoid site ( $O_2-A_1$ ).

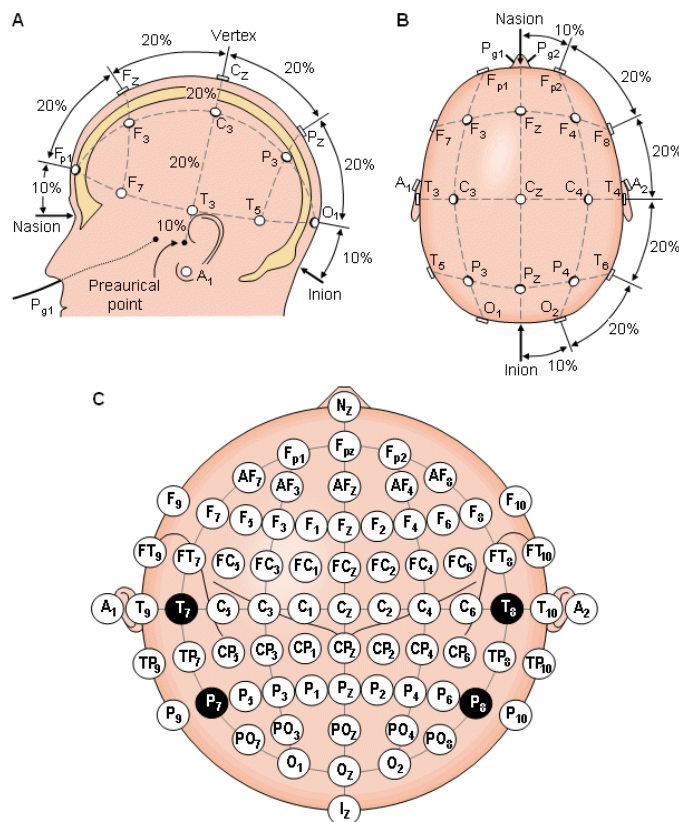


**Fig.1.2.** International 10-20 system (A) Left (B) Right (C) Location and Nomenclature of intermediate 10% electrodes as per standards of American Electroencephalographic society

**1.3.2.2. EOG.** An approach to measure the corneo-retinal standing potential (CRP) which exists between the front and back of the human eye is electrooculography. Electrooculogram is the signal obtained during this process. Eye acts as a dipole in which anterior pole acts as positive while the posterior pole acts as negative. Hyper polarization and de-polarization are produced by the nerve cells of retina generating the CRP. The CRP is oriented along the line of sight and ranges from 0.4 to 1 mV.

Localizing the eye to a remote area and if an electrode was within the proximity of the eye, the electrode turns positive when the eyeball rotates towards it and shows less positive if it rotates away from electrode.

In general there are two methods to draw the readings of the eye movements based on the position of electrodes around the eye. For horizontal movements (monocular) the electrodes are placed at the outer and inner canthi of each eye. For vertical movements they are placed above and below the eye. The potential difference between these electrodes gives the CRP. This potential is directly proportional to the electrical axis of current eye position and of primary eye position. There might be a linear relationship between them up to  $30^\circ$  corresponding to 15 to 20  $\mu\text{V}$  per degree of eye rotation [19].

EOG is used for monitoring the slow, rolling eye movements that occur during various stages of sleep. Two channels are usually used in determining the EOG. One of them is placed 1cm above or below the outer canthus of the eye. For the sake of equal amplitudes due to the conjugate eye movements the electrodes are displaced equally. Typically the reference electrode is the ear mastoid site ( $A_1$ ).

**1.3.2.3. EMG.** Electrical response due to the muscle contraction of neuromuscular activity is the electromyographic signal. The body movements are controlled by the central

nervous system (CNS) by the motor neuron through which the functioning of the body and mind occurs. The muscles are activated by the CNS through the motor neuron in which the muscle contraction takes place preceded by depolarization (sudden change within a cell when it undergoes dramatic electrical change) of the outer muscle-fiber membrane. Electric field is created by the respective motor unit (MU) where the depolarization occurred in their respective fibers. This voltage distribution on the skin is generated due to the electric field produced by these MU's. The sum is weighted by the distance of each source from the skin.

This voltage can be acquired using a pair of electrodes are placed per muscle on the skin. The difference between these two potentials is recorded for analyzing the signal. Surface electromyography (sEMG) is electromyographic signal that is encapsulated by means of couple of electrodes placed on the skin (across various parts of body in order to obtain the respective EMG signals from the particular part of the body). Response from the muscle contraction can be detected by the electric potential produced over the skin. The corresponding measure of the potential is the sEMG. Conventionally sEMG have a spectral range of 10 to 450 Hz with amplitudes up to 5mV depending on the particular muscle [20]. The travelling potential is detected with a temporal delay which depends on fiber conduction velocity if the electrodes are placed on the skin parallel to the muscle fiber.

Muscle tone is determined based on the EMG activity over the chin area. This channel acts for proving the supplementary information regarding the movements of the patient during the sleep and can be helpful in distinguishing some artifacts. In three electrodes, one electrode was placed in the midline 1cm above the inferior edge of the mandible, one submental electrode placed 2 cm below the inferior edge and 2 cm to the

left of the midline and other submental electrode placed 2 cm below the inferior edge and 2 cm to the right of the midline.

All the electrodes are placed on the methodology discussed in 1.1.1. The amplifier settings and calibration for the equipment are done based on the American Academy of Sleep Medicine (AASM) standards [7]. The scoring of each stage of sleep is discussed earlier in the sleep stage based on the EEG 1.1.3.1.

The methodology used in the sleep centers is little be uncomfortable because they need to carry many wires on their body which are fixed using adhesive tapes and gels during their sleep. These parameters might interfere with the normal sleep that an individual will have every day and might lead to erroneous diagnosis. Moreover the cost for the diagnosis in the sleep center for one night is around \$2500 which is a bit costlier approach and the person need to wait at least 2 weeks to have his turn for the diagnosis after the reservation.

#### **1.4. PORTABLE DEVICES FOR HEALTHCARE**

With an increase in number of people suffering from sleep disorders there is a demand for the number of sleep centers as the number of beds available in these health centers is limited. Moreover treating such type of disorders became an expensive to the healthcare budget. An alternative in order to meet the demand for sleep studies based on clinical diagnosis is to have a sleep study in their houses using portable devices. Home-based sleep studies are more economical as they need not effort to sleep in the healthcare centers and they can sleep more comfortably in the house and the diagnostics will be more proper.

There is lot of ongoing research in portable devices for the sake for home based monitoring. For instance *BresoDx<sup>TM</sup>* a portable acoustic device can be used as home diagnosis for people suffering from sleep apnea [21]. Another research for home based diagnosing for obstructive sleep apnea syndrome using a watch *PAT 100* a portable device based on atrial tone (PAT) signal [22]. The development of multichannel home sleep testing by a variety of manufacturer's cost-effective and highly reliable method of screening for many sleep disorders. *Embletta PDS* that measured airflow through a nasal cannula connected to a pressure transducer, oxygen saturation plus both respiratory and abdominal movements via built in-in effort and body position sensors [23]. Similar type of portable devices are available in the market and can be used in the homebased sleep studies as many of them are validated and are recommended by the practitioners and doctors [24-26].

These portable devices are similar to the devices available in the clinics and might need a medical practitioner to monitor these devices. Even though the portable devices are easy to carry, they are not quite comfortable to wear and sleep. The devices available in the market usually have the capability to diagnose some particular type of disorders and cannot have the functionality to diagnose all kinds of sleep disorders. Lastly, these devices costs around \$5000 and everyone cannot afford to use them. Hence, there is a need for a device that can be easy to wear, use and should be affordable. The device should be novel in order to analyze the data and use it afterwards as the data obtained from the diagnostics cannot be understandable to everyone. In order to treat the patient, the data received from that device needs to be sent to the clinic for the diagnosis.

## 1.5. ART OF WEARABLE DEVICES

Increase in number of chronic diseases is increasing in the world in order to monitor and treat these diseases the cost of health care is also increasing accordingly. So with the advance in the technology many researchers' and global corporate companies considered this as an issue and came up with the idea to miniaturize these portable devices to the quotidian essentials, wearable devices, to track their health and monitor their fitness regularly. The demand for these wearable devices is continuously increasing in today's society.

Innovations in such wearable technologies became as a boon for many geriatric people and people suffering from many chronic diseases who require continuous costly hospital diagnostics for their treatment. Wearable devices decreased individuals from hospital monitoring to homebased monitoring. These tele-home health monitoring devices enhanced the productivity, popularity and handling of medicines from home. These wearable devices have the qualities of working in long-term, persistent and unhampered tracking the physiological data like bio potential, heart rate (HR), photoplethysmogram (PPG), respiration, blood oxygen saturation ( $\text{SaO}_2$ ) and blood pressure (BP). Moreover these devices allow knowing more about real-time monitoring of the individual health which is not possible from hospital settings.

Typical health monitoring devices in general are wireless and serve the purpose of procuring the data like bio signals and body motion signals. A remote terminal can be used to capture signals which are processed to a nearby intermediate terminal. These preprocessed signals are sent to the smart devices as shown in the block diagram (Fig 1.3).

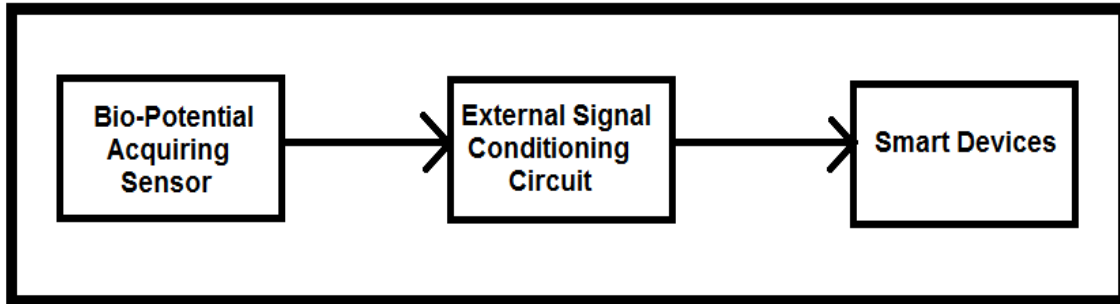


**Fig.1.3.** Block Diagram of a Typical Wearable Device

The data obtained can be increased the coverage by linking them to a network. In personal health monitoring wireless body area networks have great potential in usage of intelligent sensors for various applications like Electro Cardiogram (ECG), Electro Encephalogram (EEG), Electro Occulography (EOG), etc. Such sensors acquires signal followed by pre-processing of real-time and low level signals and communicates with the same personal server wirelessly typically these signals are further processed and stored using a mobile gateway.

Innovations are being done on this field. Some instance like '*TICKR Heart Rate Monitor by Wahoo Fitness*' the strap which allows the individual to monitor his or her heart rate measurements when he wounds the strap across his chest and the data is sent to the smart phones via Bluetooth [27]. *SOMNOwatch<sup>TM</sup>* [29] was designed in order to diagnose actigraphic data for patients suffering from sleep disordered breathing. Advanced research in wearable devices for gaze detection and eye tracking using EOG signals through different types like *Wearable EOG Goggles* [30], full-time *Wearable Headphone-Type Gaze Detector* [31] which can be helpful in human computer interface (HCI). On the basis

of surface EMG's many applications like input to the mobiles based on gestures [32], wearable EMG based HCI for wheel chairs users [33] and many more.

Most of these commercial fitness tracking devices measure the number of calories burned, distance they have covered (number of steps) and some of them time spent in the each sleep stage. Some popular trackers such as '*Fitbit Force*' and '*Jawbone UP*' use to insight the users about their sleep stages i.e. like from light sleep to deep sleep. '*Basis B1*' was different one that aims in the measure of REM sleep in addition to those fitness trackers that can monitor the sleep stages. Experts are skeptical about the accuracy of such fitness trackers that can measure the sleep.

Most of the trackers use sensors called accelerometers for detecting the motion of the body like direction and speed. These trackers theoretically give information to the users whether they are awake or sleeping but it involves many practical mistakes. So the results obtained from such trackers are not appropriate for diagnosing the sleep disorders and are futile for clinical purposes.

Montgomery-Downs [28] conducted a research in 2011 comparing the results obtained from standard polysomnography to the sleep monitoring based on fitness trackers. They observed the fitness trackers overestimated an individual asleep around 67 minutes (Fitbit), 43 minutes (ACTi graph), etc. Most of the devices showed that the person is asleep even when the person is not sleeping. Sleep scientists generally use EEG, EOG and muscle tone in order to conclude about the various stages of sleep.

Healthy people using these devices to track their sleep doesn't create a problem for them but if a person with sleep disorder believing this data may be a potential danger as they are using just data based on accelerometers instead of EEG, EOG data. There is a need



to have wearable device that can help in monitoring the various stages of sleep using EEG, EOG and EMG.

## **1.6. NOVEL DEVICE FOR EPIDERMAL INTEGRATION**

Epidermal devices are one kind of wearable devices. From the previous sections it is observed that there are many health monitoring wearable novel devices but none of them satisfy the required demand in order to have a health monitoring device that can be used outside the clinic. The conventional methods used in the clinics for sleep disorder diagnoses involves flat electrode pads which involves placing them over a small number of points using conductive gel in order to minimize the number the contact impedances. This approach cannot be followed regularly as the gels may not be compatible for everyone's skin, creates discomfort for the people requires several clinical sittings or may loss adhesion for people with unfavorable skin-electrode interface [35].

Considering the backdrops of the clinical treatment, the device required should be different from the conventional method of testing used in sleep centers i.e. it should be minimal invasive, should use minimum number of gels, minimum number of electronic devices to be placed on the skin, etc. Many technological works [34] in health and wellness monitoring proved that fully integrated electronics that are soft and stretchable can resolve the problem. Such devices are adhered with a basis of a membrane to intimate variety of electronic and sensor technology directly with the skin using the vander wall forces to measure the electrophysiological signals (EP) generated by the body. This membrane should behave similar skin mechanical properties so that it is robust, free from mechanical constraints to capture the EP signals, has non irritating skin/electrode contact.

Skin has several layers within the body for convenience consider it as a bilayer, with epidermis of approx. 0.05 to 1.5 mm thick and dermis of approx. 0.3 to 3 mm thick as shown in Fig 1.4. Moduli of these layers are about 140 to 600 kPa and 2 to 80 kPa of epidermis and dermis respectively [34]. This bi-layer of skin responds about 17% of tensile strain for linear elastic and more than 30% non-linear irreversible at higher strains. In practice the skin is not smooth which has many wrinkles and has many irregularities like creases and pits of 15 to 100  $\mu\text{m}$  & 40 to 1000  $\mu\text{m}$  respectively.

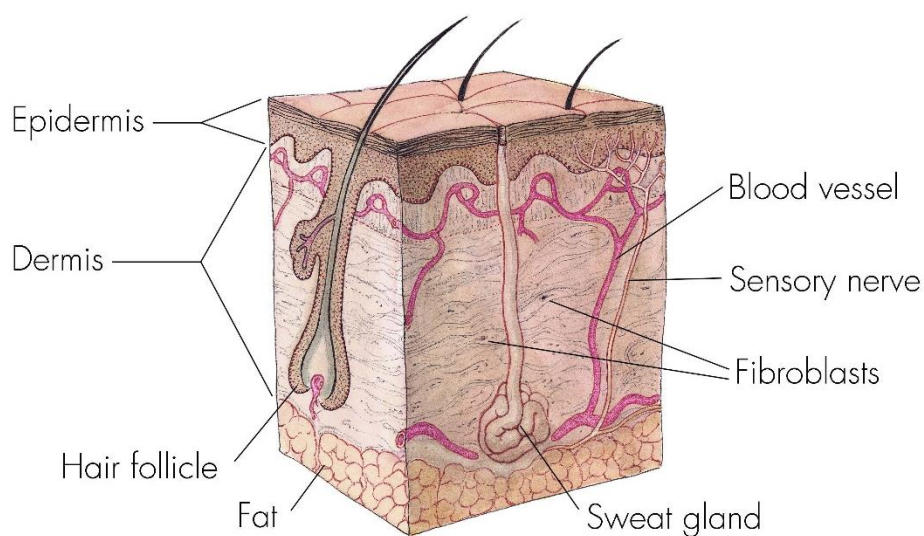


**Fig.1.4.** Side View of Layers of Human Skin

To reach the above requirements the membrane should be with low-modulus, lightweight, ultrathin, stretchable skin like membranes on which all the electrodes, sensors

and communication parts are placed together to measure the corresponding potential across that particular position of the skin. As the membrane is with the physical properties of the top layer of the skin this class of devices are called epidermal electronic systems (EES). EES are used to measure the EP signals like ECG, EEG, EOG, EMG, as well as temperature, mechanical strain, sweat levels, hydration of the skin, power source and can also act as a human computer interface [34-45].

Biological tissues are soft curved and textured which are different from the conventional bio medical sensors as they are typically rigid, planar and use metal electrodes. Hence, there was variability in the point of electrode and tissue contact. There was a significant difference in accuracy and precision. For enhanced conformability these biological tissues should have a textured surface and affixed to the skin by a soft contact, they are made on the basis of dry electrodes that are made of ultrathin pliable polymer films and elastomer substrates offer improved capabilities. Such epidermal devices can be intimated to the skin by Vander walls force because of their mechanical properties (thermal loads, area mass densities and thickness) similar to dermis.

The necessity of using additional straps, pins and tapes are eliminated as the device can be attached based on the London-dispersion effect between the skin and the elastomer substrate. This advantage of contact provided a window for monitoring the overall health status based on the measurement through internal body process as they are precise and repeatable.

## 2. DESIGN AND FABRICATION

### 2.1. DESIGN OF THE SENSOR

The principle ideology for a sensor in this study is its capacity of detecting and transmitting electrical waves within a specific range of frequencies. As it needs to be coupled with the skin during the recording of the physiological signals it should be compliant, flexible and stretchable. One best approach to meet this requirement is to design the sensor in the serpentine structure as it provides those qualities with its design. It is a multi-layered sensor with each layer serving a functional purpose. Fig 2.1 shows the functional parts of an EES, epidermal sensor for this project. It consists of thin filamentary serpentine (FS) connected with a FS layout to measure EP signals and strain sensor to use as a part of sleep study.

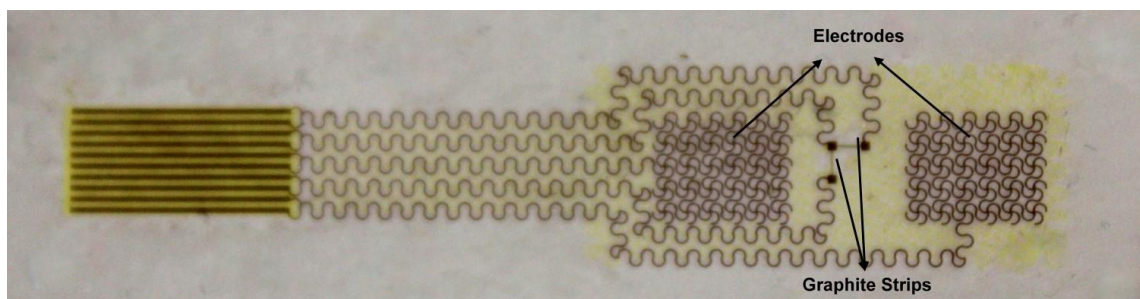


**Fig.2.1.** Functional parts of the epidermal sensor

Usually these types of circuits have a high deformability and low effective elastic moduli. These EES devices orient naturally to the skin's contoured surfaces and time-dynamic motion because of its design. A layout of FS arranged in an order to obtain the EP signal from the skin Fig 2.2 and Fig 2.3 shows the view of a single EP sensor (200  $\mu\text{m}$ ) & graphite strips (500  $\mu\text{m}$ ) respectively, when observed under an SEM. There are two FS layouts made of copper for obtaining the potential and the difference between them gives the differential bio-potential at that point on the skin. There are three nodes connecting two graphite strips, the intersection node is the common node or the ground for both of the strips. Fig 2.4 illustrates the exploded view of various layers of the sensor.

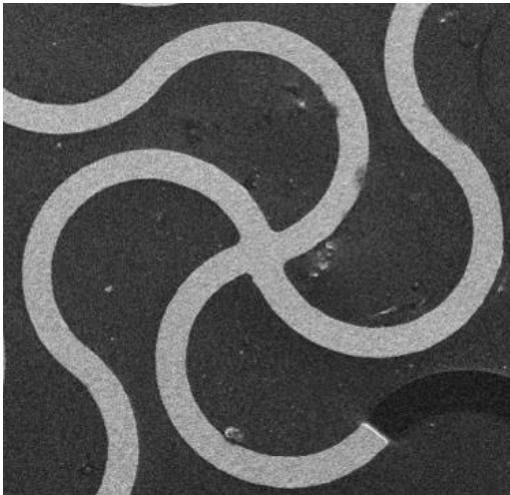


**Fig.2.2.** EP sensor when observed under an SEM at (200 $\mu\text{m}$ )

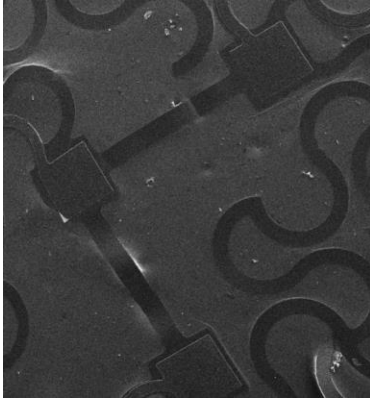


**Fig.2.3.** Graphite strips on the EES under an SEM (500  $\mu\text{m}$ )

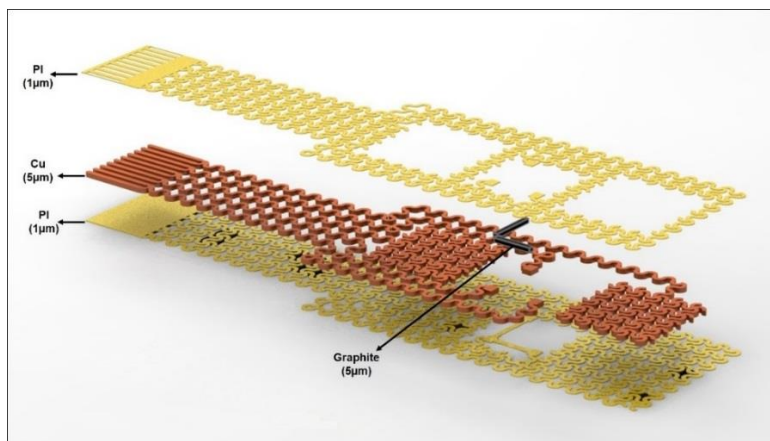


**Fig.2.4.** Exploded view of the schematic diagram of the sensor

The entire sensor consists of three layers in which the middle or neutral mechanical plane (NMP) consists of all the active sensing components and interconnect wiring while upper and base layers are made using polyimide (PI 2445, 1  $\mu\text{m}$  in thickness, HD microsystems, USA) to protect the NMP. The NMP consists of copper electrical

interconnects and graphite strips, copper FS layout acts as an EP sensor while the graphite strip acts as a strain gauge. All the sensors parts in NMP are connected to the contact pads via FS. The contact pads act as data transfer pivots for the EP sensor. The two graphite layers act as strain gauges that generate signal based on differential mechanical kinematics of the skin surface. Bending-induced strains are minimized due to design of the device. A schematic sensor's exploded view is shown in Fig 2.4. The total thickness of the sensor averages at 7  $\mu\text{m}$  across the thickest part which is fifty times thinner than the human epidermis.

## **2.2. SILICONE MEMBRANE FOR THE SENSOR**

With the help of a substrate, the sensor is coupled with the skin surface. There is a layer of adhesive over the substrate as the sensor needs a means to stay on the substrate, which should be biocompatible on the skin as discussed earlier in previous sections. Moreover, it should be as thin as possible to avoid minimal sensations and irritations on the skin surface. It should be flexible enough to support the sensor to expand or compress. It should stay long on the skin to maintain the device on the skin. It should be placed easily and can be removed easily from the skin.

Elastomers like PDMS (Sylgard 184 Elastomer Kit, Dow Corning Corporation, USA), Mold Max (Mold Max 20, SMOOTH-ON, USA) and Dragon skin (Dragon skin slow, SMOOTH-ON, USA) are chosen to serve for the silicon base. All these materials can be used for the current purpose but due to the transparent color and high stretch ability of 'Dragon skin', was chosen. This silicone membrane needs an adhesive layer to hold the

device or to stay on the human skin. Silicon adhesive (SILBIONE RT Gel 4317, Bluestar Silicones, USA) is a biocompatible and non-irritating material for human skin.

A backing layer is required for the purpose of preparing and removing the silicone membrane from the glass slide. There are various suitable backing films but a dominant consideration is a backing film which could be peeled from the silicone easily. Initially two different backing layers (1-Scotchpak<sup>TM</sup> White Backings and Release Liners, 3M, USA & 3M Scotchpak<sup>TM</sup> Release Liner Fluoropolymer Coated Polyester Film, 3M, USA) are proposed due to their biocompatibility, inert behavior in responding with the materials and can be removed easily from the materials due to their smooth surface. During the actual practice, only the second film has been chosen because of its transparency.

Initial iterative trials were performed; the film didn't serve its current purpose of peeling the backing film efficiently, i.e. without disturbing any of the three silicon membranes. Therefore, a buffer layer with a lubricant was added, which again should be non-irritating to the skin and biocompatible. So natural oils (coconut oil, olive oil) were used. Two (Mold Max 20 with any of the backing films using any buffer) out of 6 possibilities (3 types of silicone materials with 2 different lubricant layers) showed better response and were not up to the mark in the initial trials look Table 2.1.

Even the mold release agent (Ease Release 200) did not give a good response as a buffer between the backing and silicon because of its non-uniform behavior of spreading over the backing layer. A slight rough surface film (Acetate Sheet, Grafix Plastics, and USA) gave an unhindered solution even without the use of a lubricant. The force required to peel the backing film using the acetate film gave very good results considerably when compared with the previous cases shown in Table 2.1. Fig 2.5 illustrates various layers of



the silicone membrane. Table.2.2. specifies the force required to peel the acetate film from various silicone membranes.

**Table.2.1.** Maximum force required to peel the backing layer (3M Scotchpak™ Release Liner Fluoropolymer Coated Polyester Film, 3M, USA) with different lubricants as buffer.

	No Oil	Coconut Oil	Olive Oil
PDMS	44.72 N	20 N	16 N
Mold Max	12 N	3.8 N	2.5 N
Dragon Skin	15 N	4.2 N	3.2 N

**Table.2.2.** Maximum force required to peel the acetate film from various types of silicon membranes.

	Force (N)
PDMS	0.48
Mold Max	0.26
Dragon Skin	0.15

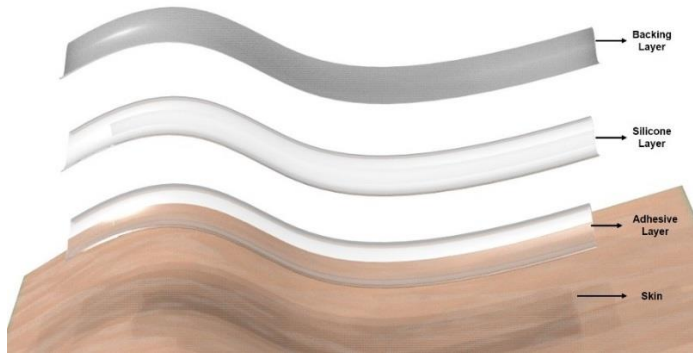


**Fig.2.5.** Exploded view schematic diagram of the silicon membrane for the sensor

The final snag was the un-curing of the silicon adhesive over the silicon membranes due to the smooth surface of the silicon layer that was overcome using plasma etcher to make it rough.

### **2.3. FABRICATION TECHNIQUES**

The steps involved in the fabrication of the epidermal sensor typically deals with preparing the sensor and silicone membrane and transfer printing the sensor over the silicon membrane. Fig 2.6 illustrates a schematic diagram that involves the list of steps involved in fabricating the device.

The glass slides were cleansed using Acetone and Isopropyl alcohol to get rid of the organic and inorganic particles. The process starts by spin-cast of polydimethylsiloxane (PDMS,) mixed at a ratio of 10:1 (base: curing agent) by weight onto a clean glass slide at 500 rpm for 45 sec and cured at 120<sup>0</sup>C for 20 min (see Fig 2.6. (a)).

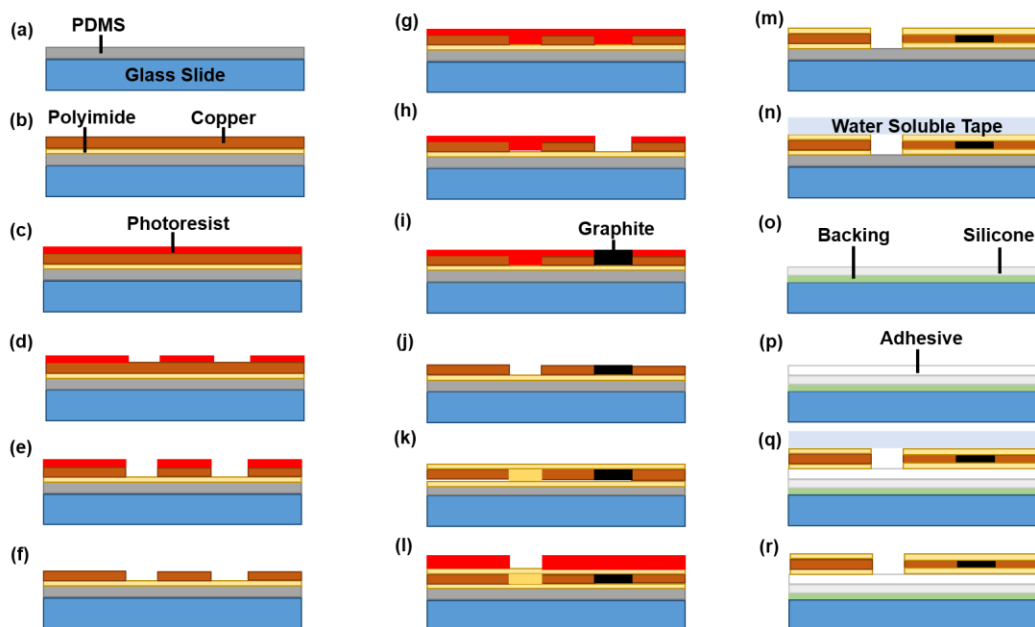


**Fig.2.6.** (a) to (n) Schematic illustration of steps for fabricating epidermal sensor. (o) to (r) Epidermal sensor mounted on the silicon membrane

The copper film consists of two layers one with 5  $\mu\text{m}$  and other with 40  $\mu\text{m}$ . To have 5  $\mu\text{m}$  copper film, the copper film was taped with 5  $\mu\text{m}$  facing top and spin coat the polyimide at 3000 rpm for 45 sec. It will be pre-cured for 5 min at 180 $^{\circ}\text{C}$  followed by post-curing for 90 min at 250 $^{\circ}\text{C}$ . After the Polyimide is cured the thicker copper layer of 40  $\mu\text{m}$  is removed by placing the polyimide layer facing towards the PDMS layer of the glass slide (see Fig 2.6. (b)).

A layer of photoresist (AZ P 4620, AZ Electronic Materials, USA) has been spin-casted at 3000 rpm for 45 sec and cured at 120 $^{\circ}\text{C}$  for 3min, followed by exposure (using a mask that has patterns for the copper layer) and developing the sample (see Fig 2.6. (c), (d)). The copper layer when wet etched in shape of the developed layer of photoresist by

dipping the sample in the copper etchant until the unexposed part of the copper has been etched and the photoresist is removed (see Fig 2.6. (e), (f)).

The second layer is again spin-cast, exposed (with a mask that covers the entire copper film except the graphite strips) and developed using the same parameters used for developing the copper layer, the graphite powder is swirled in the slots present in the copper pattern which has been developed followed by the removal of photoresist (see Fig 2.6. (g) to (j)).

Third layer, polyimide, is spin-casted (same parameters used for spin casting and curing the first layer of polyimide) over the sample. Followed by spin casting of two thin layer of photoresist (first layer with 3000 rpm for 45sec and cured at 90<sup>0</sup>C for 3 min, while the second layer with 1000 rpm and cured for 120<sup>0</sup>C for 3 min). The sample was exposed (with a mask that covers the entire copper layer except the parts to be touched by the skin and the contact pads to connect to the external circuit) and developed (see Fig 2.6. (k) to (l)). The entire polyimide layers are dry etched using the plasma etcher (Plasma Etch, USA) and the processed sensor is picked up from the PDMS glass slide using a water soluble film (Water soluble tape, Aquasol Corporation, USA) (see Fig 2.6. (m), (n)).

A separate glass slide with backing film is affixed by taping its edges for preparing the silicon membrane. The silicone membrane (Dragon skin slow, Part-A and Part-B mixed in a ratio of 1:1, Smooth-On, USA) is spin-casted at 3000rpm for 45 sec and cured (see Fig 2.6. (o)). The silicon layer is dry etched in a plasma etcher to make the top layer of silicon membrane rough and the silicon adhesive is spin-casted at 2000 rpm for 45 sec and cured at 120<sup>0</sup>C for 5 min (see Fig 2.6. (p)).

The device with water soluble film is placed on the adhesive layer of the silicon membrane (see Fig 2.6. (q)), the water soluble film is removed by dripping distilled water (see Fig 2.6. (r)) proceeded by cleaning the device with nitrogen gun. Fig 2.7 illustrates the schematic representations of all the layers of the device. The device is ready to pair with the skin and soon after the removal of the backing layer, testing is initiated. Fig 2.8 shows the transfer printing of the device to a water-soluble film while the Fig 2.9 and Fig 2.10 shows the flexibility and twisting of the device on the silicone membrane respectively.

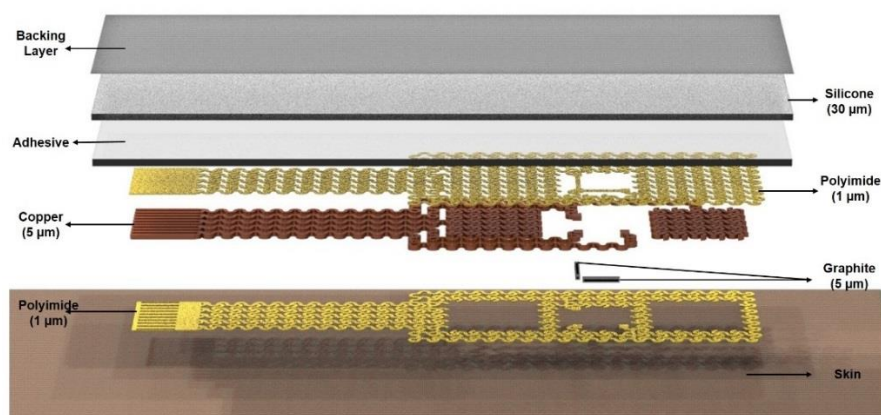


**Fig.2.7.** Schematic exploded view of all the layers of the device

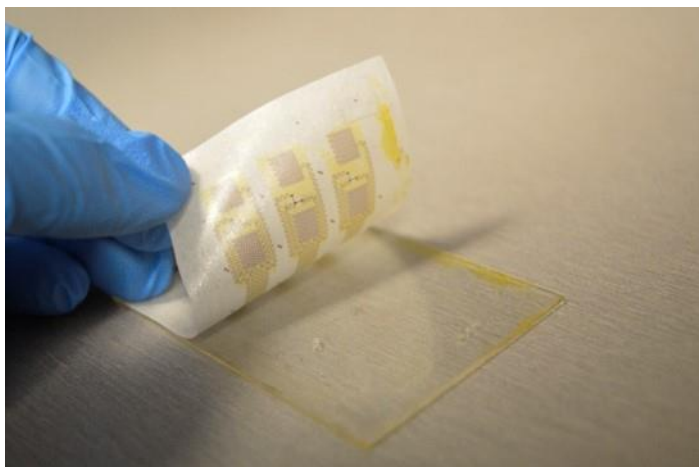


**Fig.2.8.** Transfer printing of device from glass slide to water-soluble film

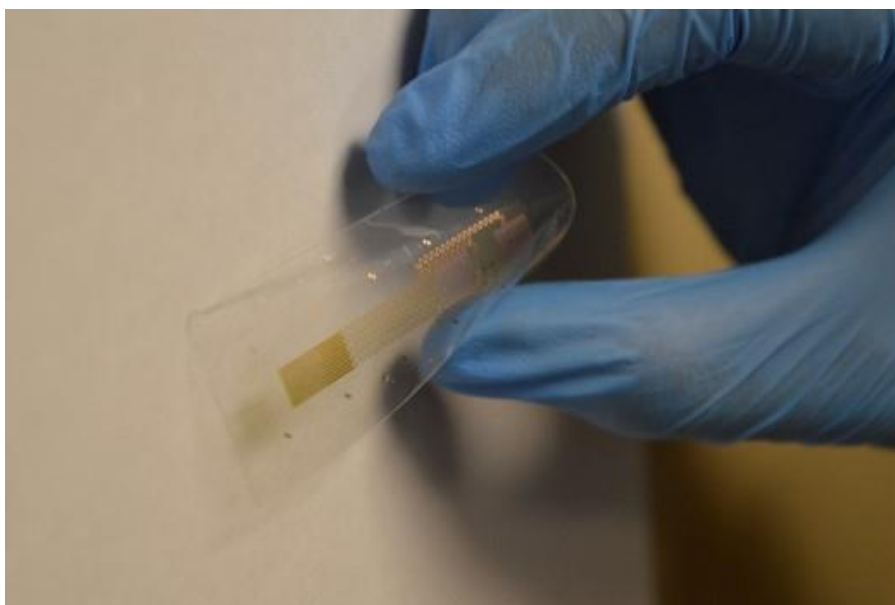


**Fig.2.9.** Flexibility of the device on the silicone membrane

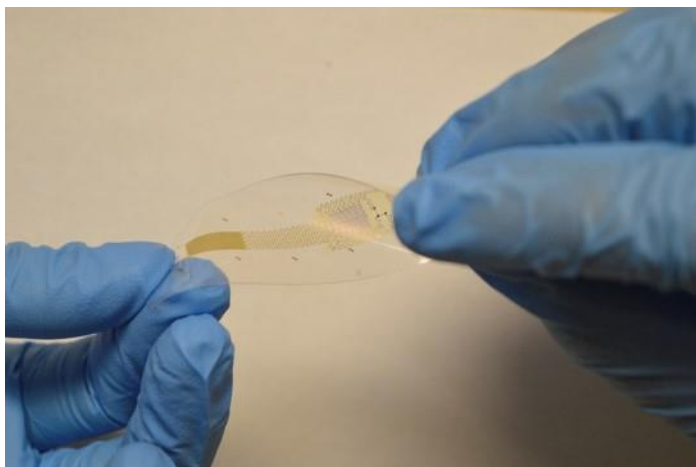


**Fig.2.10.** Twisting of the device on the silicone membrane

### 3. EXPERIMENTAL SETUP & METHODS

#### 3.1. PARAMETERS REQUIRED FOR SILICONE MEMBRANE TO MOUNT ON THE SKIN

One of the salient features of the device is its ability to pair with the skin for data acquisition. Silicone membrane has a property to elongate with the device and should not be a constraint when the device needs to elongate or compress when subjected to mechanical skin dynamics. As discussed in the previous sections the membrane has three layers as shown in Fig 3.1.

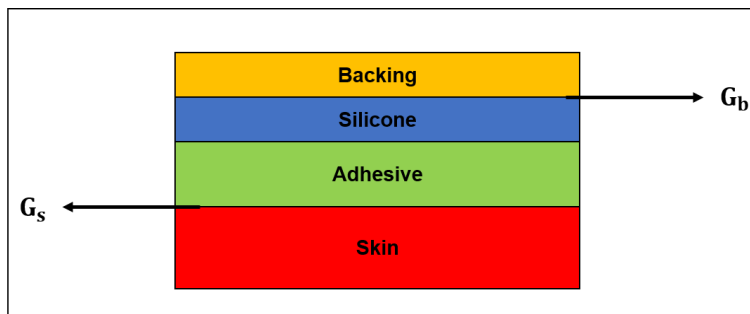


**Fig.3.1.** Layers of Silicone Membrane

In order to pair the device to the human skin the backing layer needs to be removed with delicate care for other membranes, which is vital for effective functionality of the membranes. If  $G_b$  is considered as the adhesive energy between the acetate film and the silicone layer; and  $G_s$  is the adhesive energy between the silicone adhesive layer and skin.



In order to satisfy the requirements for safe handling of the membrane during the peeling of the backing layer is shown in (1).

$$G_s > G_b \quad (1)$$

$G_w$  is the working energy required to peel the membrane and the corresponding condition is depicted in (2).

$$G_s > G_w > G_b \quad (2)$$

A common approach for measuring the interface mechanical adhesive properties is by a peel test. The primary principle involved in calculating the energies are energy balance approach using fracture mechanics. Several assumptions are considered in doing the peel test like the inextensibility of the acetate tape when it is peeled from the silicon layer (Kendall, 1975) and the elastic energy term is neglected during the energy balance approach. However this term is considered during the peeling of elastomer from the skin as it is considered to be an extensible linear elastic medium [46].

**3.1.1. Background.** Consider a peeling of an elastic thin film from a rigid substrate as shown in Fig 3.2. The variables to be considered are thickness of the film  $d$ , width of the film  $b$ , force to peel  $F$ , the extension  $\delta$ , angle with which the film is peeled out from the substrate  $\theta$ , length of the peeled portion of the tape is  $c$ , length of the film to be peeled is  $\Delta c$  from point A to B.

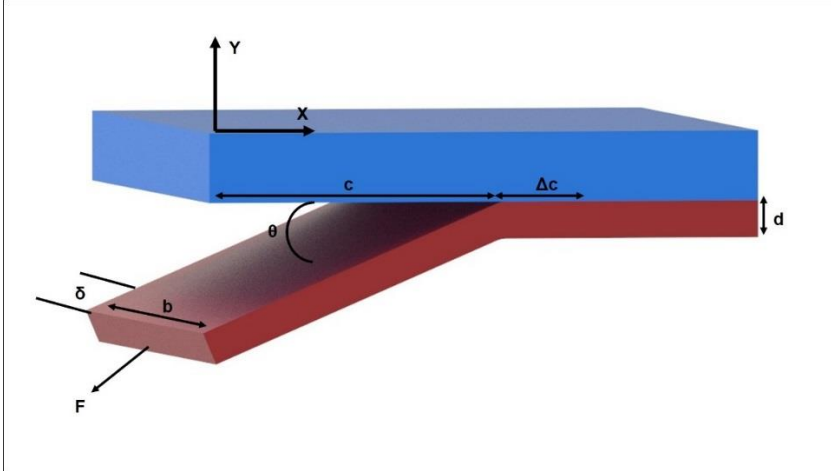


**Fig.3.2.** Elastic film peeling from a rigid substrate

If the energy balance is considered during the process the external work done by the system is equal to the internal energy stored.

$$W_p = U_e + U_s \quad (3)$$

Where  $W_p$  is the amount work done to peel the film from A to B,  $U_e$  is the elastic energy stored in the film due to the extension of the peeled portion  $c$ ,  $U_s$  is the surface energy to create the two surfaces. Assuming the linear elastic film with constant width and thickness, the extension of the tape in the peeled region and elastic energy equations are given in (4) and (5) respectively.

$$\delta = \frac{F\Delta c}{Ebd} \quad (4)$$

$$U_e = \frac{1}{2}F\delta = \frac{F^2\Delta c}{2Ebd} \quad (5)$$

E is the young's modulus of the film. According to the fracture mechanics the surface energy is analogous to fracture energy to create new surfaces during peeling. Then surface energy is shown in (6).

$$U_s = -b G \Delta c \quad (6)$$

Where G is the thermodynamic adhesive energy required to fracture a unit area<sup>[47]</sup>. When the force is applied on the film the force  $F$  moves a distance of  $\Delta c (1 - \cos\theta) + \delta$  from the initial position the change in potential energy due to this force is the external work done  $W_p$  and is given by (7).

$$W_p = F (\Delta c(1 - \cos\theta) + \delta) \quad (7)$$

Substituting (5), (6) & (7) in (3) and solving for G in the Kendall equation as shown in (8) gives.

$$G = \frac{F^2}{2Eb^2d} + \frac{F}{b}(1 - \cos\theta) \quad (8)$$

If the film is inextensible then the elastic energy term is neglected and popular known for Rivlin equation as shown in (9).

$$G = \frac{F}{b}(1 - \cos\theta) \quad (9)$$

Equation 8 & 9 represents the energy terms to find the adhesive energy between the layers. In order to find the energy required to peel one layer from the other, the force required to peel is not a steady state force. To find the working force, the model as shown in Fig 3.2 was taken into consideration. A thin film will be stripped from a rigid substrate this thin film is infinitely stiff in the axial direction. The adhesive fracture energy [48] is given by equation (10).

$$G_c = \left( \frac{dU_{ext} - dU_s - dU_d - dU_k}{b dc} \right) \quad (10)$$

$b dc$  is the incremental area created during the peel test,  $G_c$  is the adhesive fracture energy,  $dU_{ext}$  is the incremental external work performed which is  $F dc (1-\cos\Theta)$ ,  $dU_s$  is the change in stored strain energy,  $dU_d$  is the increment of dissipated energy other than creating new surface,  $dU_k$  is the incremental change in kinetic energy. The equation used in (10) is to determine the amount of working force that can peel the acetate film from the silicone membrane. As the membrane does not store or dissipate energy during the peel test  $dU_s$  &  $dU_d$  are zero (acetate tape is infinitely flexible & inextensible during the peel test).

The speed with which the membrane peels out is the important parameter that needs to be considered if the test speed is  $V$ . If the velocity components of the peeled arm are  $V (1-\cos\Theta)$  &  $V (\sin \Theta)$  then the incremental dissipation energy per unit area is given in equation (11).

$$\frac{dU_k}{b dc} = \rho d v^2 (1 - \cos \Theta) \quad (11)$$

Where density of the arm is  $\rho$  and peeling speed is  $v$ . Equation (12) gives the total energy required to peel backing layer from the silicone membrane.

$$G_c = \left( \frac{F}{b} - \rho d v^2 \right) (1 - \cos \Theta) \quad (12)$$

**3.1.2. Experimental Setup.** Peel test between various layers in order to determine the respective energies between the layers. The peel test is conducted using a mini tensile tester with a force gauge (Mark-10) as shown in Fig 3.3.

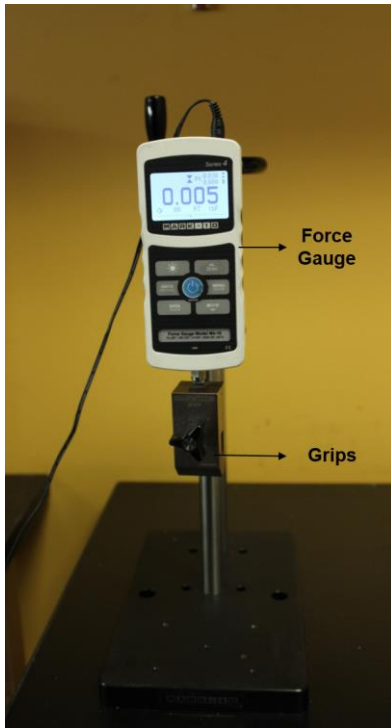


**Fig.3.3.** Mark-10 Force Gauge

Firstly in order to find the  $G_b$ , a silicone membrane is fabricated as per the procedure mentioned in the previous sections. The membrane is cut into a square (25 mm  $\times$  25 mm) in dimension in order to conduct the peel test. Now the layers are cut and transferred onto a glass slide such that the acetate tape faces the top layer and the adhesive is attached to the glass slide and is affixed on a fixture with the help of two vertical clamps to hold the glass slide. The other end of the adhesive tape is fixed in grips of the force gauge. A schematic representation of layers of the silicone membrane for finding the energy between silicon layer and the backing is shown in Fig 3.4. & Fig 3.5. shows the process of peeling the backing layer from the silicone membrane on the mini tensile tester. The upper grip is now set into motion manually, which starts to peel the backing layer from the silicon

membrane. The position of the membrane that has been peeled out and the corresponding force obtained are tabulated. The schematic representation of orientation of the layers for measuring the force required to peel the acetate film from the silicone layer is shown in Fig 3.4.

For measuring the adhesive energy between the silicone adhesive and the skin, a new film with same dimensions was coupled with the silicon layer paired with the skin, now the backing layer is removed as shown in Fig 3.5 and various associated parameters are noted, a schematic representation of the layers of the silicone membrane is shown in Fig 3.6. and the test is conducted as shown in the Fig 3.7. In order to measure the energy required to peel the backing film from silicone the peel test is done continuously whereas for both of the prior tests the force measured is collected for every 1 mm.

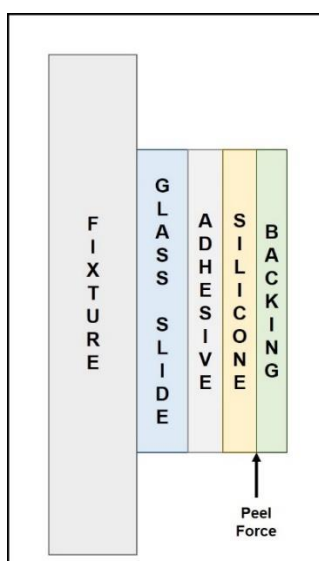


**Fig.3.4.** Schematic representation of layers of silicon membrane during the peel test for measuring the peel force between the silicone layer and backing layer.

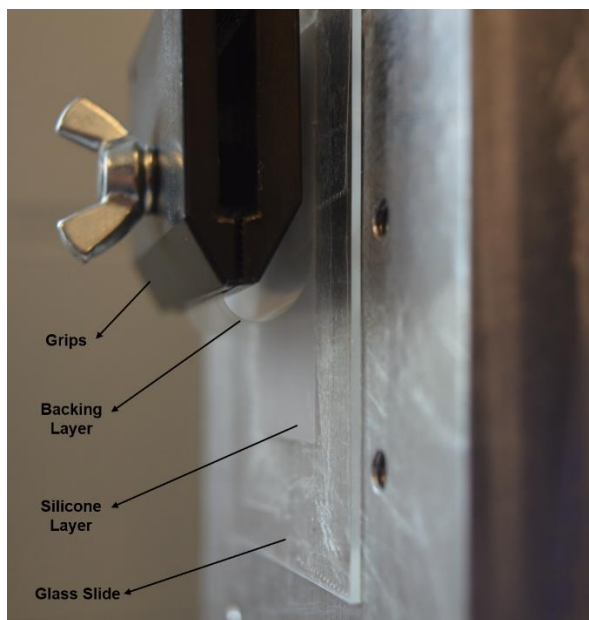


**Fig.3.5.** Backing layer being peeled from the silicone membrane on the tensile tester

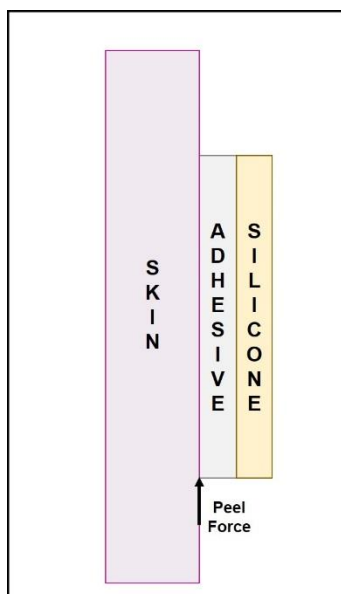


**Fig.3.6.** Schematic representation of layers of silicon membrane during the peel test for measuring the peel force between the adhesive layer and skin.

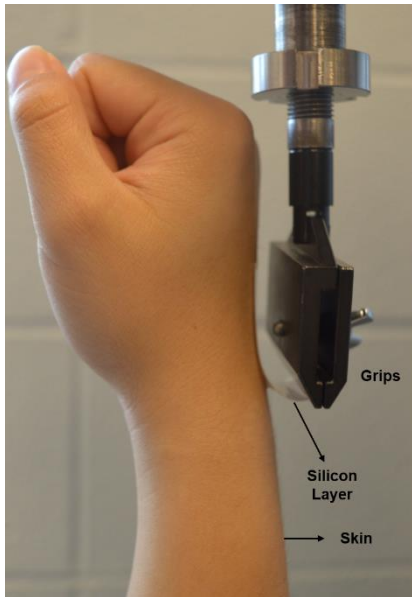


**Fig.3.7.** Peeling of the adhesive layer from the skin by the tensile tester

### **3.2. EXTERNAL SIGNAL CONDITIONING CIRCUIT FOR MEASURING THE EPIDERMAL DEVICE**

As the device is passive in nature, it needs an external source to calibrate the data that is sensed by this device. This device contains two pads that measure the differential bio-potential. These two pads are in contact with the skin the data like sinusoidal waves obtained from this electrodes is subtracted one from the other to get the differential bio-potential. The device has two graphite strips that measure the strain in two directions. There are 10 pads that connect with the external circuit for each electrode or graphite node. As the interface between the contact pads and the serpentine wires are in microns with high damage probability, so there are two pads to ensure at least one pad works if any one of



the connection is broken. The Fig 3.8. Illustrates the appropriate pad to measure their respective signals obtained from the device.

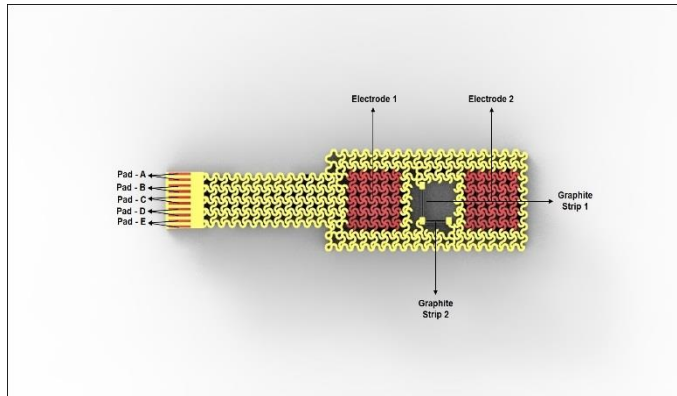


**Fig.3.8.** Nomenclature of various pads of the epidermal sensor

A commercial wireless Bluetooth circuit (BITalino architecture) is used to measure all the signals that are obtained from the device. The circuit has been modified in a way that it can measure EEG & EOG in addition to the features depicted in Fig 3.9. Maximum versatility can be achieved by modular blocks of the BITalino. The acquisition of physiological signals, the analog front-end integrates individual sensor blocks for electrocardiography (ECG), Electromyography (EMG), electro dermal activity (EDA) and accelerometry. Control blocks with micro-controller unit (MCU), power management block and a wireless communication block that uses a class II Bluetooth module (CSR chipset) serve the back-end. The specifications of the circuit are mentioned in Table 3.1.

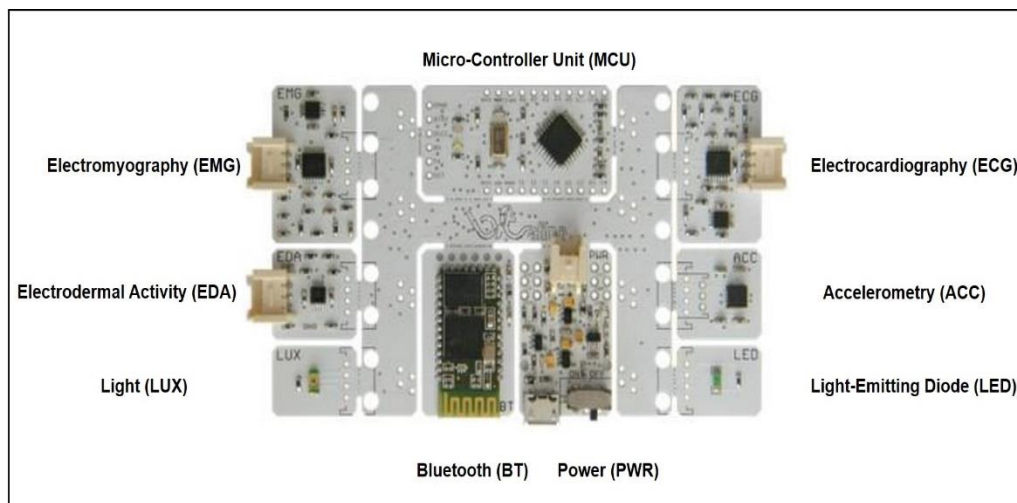


**Fig.3.9.** External Bluetooth Circuit

**Table.3.1.** BITalino specifications

	Specifications
MCU	ATMEGA328P-AVR 8-bit RISC
Clock	8MHz
Power	$V_{cc} = 3.3V$ ; $V_{ss} = 1.65 V$ ; GND = 0V
Battery	Polymer Lithium ion-3.7 V- 500m Ah
Data Link	Class II Bluetooth v2.0 (range up to 10 m)- 115200 bps [Baud]
Sensors	ECG;EMG;EDA;ACC;LUX
Actuators	LED
Weight	30 gm
Size	105*60 mm

Unfortunately, the Bluetooth circuit has been configured only to measure the signals obtained from the electrodes. For measuring the strain from the sensor, a commercial digital multimeter (DMM) for measuring the resistance of these two strips. Conductive polymer strips connects to the sensor and the PCB circuit. Typically, this PCB circuit have through holes to represent the individual pads in the PCB circuit and use only one of the pads to read the data of each function. Table 3.2. shows the mode of measuring the parameters that are obtained from the epidermal device.

**Table.3.2.** Nomenclature of the pads and their mode of measurement

S. No	Pad Name	Pad Number (Ascending order from top to bottom)	Mode of Measurement
1	Pad - A	1-2	Bluetooth
2	Pad - B	3-4	DMM
3	Pad - C	5-6	Bluetooth
4	Pad - D	7-8	DMM
5	Pad - E	9-10	DMM

In real time all the commercial DMM's have the capability to measure a single variable or single strip at a time. As it has two terminals that can measure only thing at a time. A multiplexer (mux) is used in order to select the channel required, as the device has

two inputs (two graphite strips) to measure the data. For the current purpose, a 2 to 1 mux serves in which can accept two inputs and send one output based on the selective signal. The 2 to 1 mux is very tiny and to optimize the design functionality, so an 8 to 1 mux for was chosen for current application. An 'Enable' serves the purpose of controlling the mux. It has two strips with three digital inputs and 8 different combinations corresponding to 3 of 8 channels of the mux. As pad-D is common pad for both the graphite strips it is connected to the ground in a manner pad-B gives the data of graphite strip-1 while pad-B reads the data obtained from graphite strip-2. So one of the wires from the DMM connects the output of the mux while the other is grounded.

There are many commercial ways in order to choose the signal from the mux like microcontroller, digital I/O, etc. for the current purpose, a digital I/O is used to send the selecting signal to the mux. Only one signal from digital I/O to mux is required, so it requires only 0 & 1 to select two channels. The enable of digital I/O is connected the VCC of mux which is 5V, eliminating the need of external power supply to the mux. All these devices are controlled using a laptop with the help of LabVIEW to handle the devices and record the data in the entire process Fig 3.10. shows the block diagram of the external conditioning circuit.

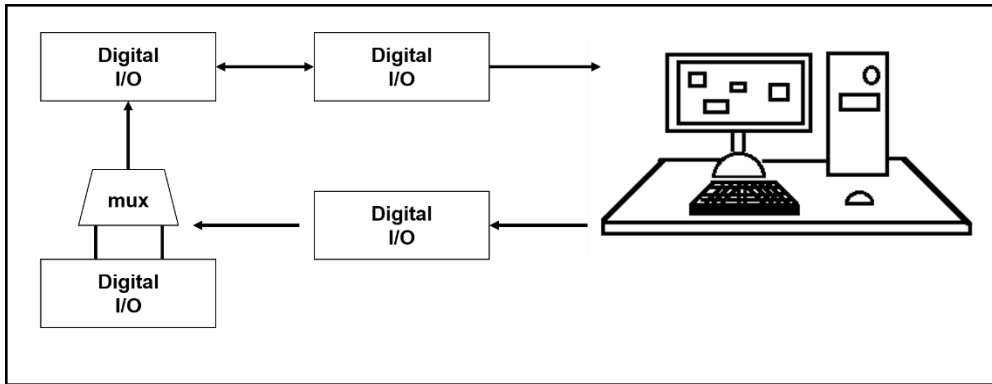


**Fig.3.10.** External conditioning circuit for the epidermal sensor to measure the graphite resistance

The DMM connects the laptop using the GPIB to USB converter. This converter allows a two-way communication between DMM and the laptop. A Digital I/O controls the mux; while the Digital I/O is configured and controlled by the LabVIEW.

Data captured from the external conditioning circuits have all the captured signals obtained from the body but it cannot be analyzed directly as it contains many artifacts like noise [49-54]. Noise components in the surface physiological signals are common and inevitable. The data analyzed using such signal may correlate to an erroneous result. The effective way of overcoming such hurdles is to filter maximum amount of noise from the data obtained. A band pass filter [49] would be very effective for the purpose, as the spectrum range for each kind of the physiological signal. The position of the sensor should be an important parameter in consideration of the noise levels while placing the electrodes over the muscle fibers that are intersecting tendons or on top of the excitation zone of a muscle the amplitude obtained would be high.

It is quite complicated to set the frequency range of high-pass corner frequency for the lower end of the signal because of many signals overlapping at this range. Contamination of the physiological signal involves many intrinsic and extrinsic parameters. Using a 60-Hz notch filter, the power line noise and cable motion artifact, which are extrinsic, are eliminated [37]. The intrinsic parameters are due to electronics of amplification systems and skin electrode interface [50]. Several organizations set different standards based on their works based on the physiological signals to have the signal free from the noise. The range of the filters to be used for different kind of EP signals are tabulated in Table 3.3 [49] [54] [37].

**Table.3.3.** Range of spectrum to set the filters for different EP signals [49] [37] [54].

S.No	Physiological Signal	High Filter	Low Filter
1	Electroencephalography (EEG)	35 Hz	0.3 Hz
2	Electrooculography (EOG)	0.5 Hz	20 Hz
3	Electromyography (EMG)	10 Hz	450 Hz

Filtering the raw data obtained from the sensors using the above spectrum range allows the user to analyze for future use.

**3.2.1. Setup for the In-Vivo Characterization of the EP Sensor.** After the sensor is transfer printed on to the silicon membrane, an ACF cable joins the contact pads to a small PCB circuit. This PCB circuit is connected with the commercial Bluetooth sensor as shown in Fig.3.11.

The differential placement of the device results in acquisition of different EP signals based on their placement location over the human body. For instance placement of device on the scalp manifests in obtaining the EEG signal, jaw manifests in obtaining the EMG signal whereas EOG is obtained by placing the sensor on any side of the temples on the human head.

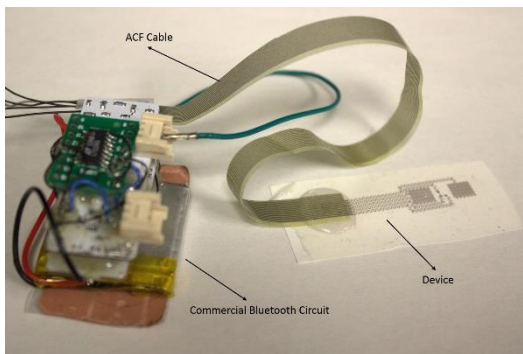


**Fig.3.11.** Setup for capturing the EP Signals

The Bluetooth sensor is turned ON and paired with the laptop with the help of the software (*Open Signals*). The significant EP signals are captured in the laptop via

Bluetooth. The raw data collected from the software is filtered using a bandpass filter (*Kaiser Win*) in MATLAB.

### 3.2.2. Experimental Setup In-Vitro Characterization of the Strain Sensors.

The capability of the strain sensors in detecting the directional strains in the skin are evaluated with a mechanical stage. In-vitro characterization is possible through the measurements conducted with the epidermal sensor on a flat glass substrate, while systematically elongating or compressing the device. The stretcher has two stations in which one is fixed and other is moving horizontally when thimble is rotated. The distance between the stations can be measured with the sleeve scale as shown in Fig 3.12.

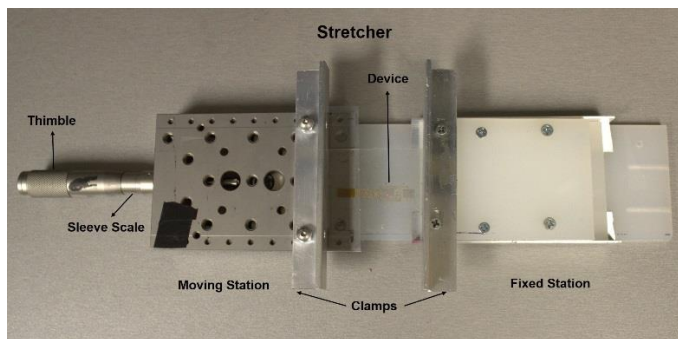


**Fig.3.12.** Device fixed on a stretcher

The sensor is transfer printed on thin PDMS membrane (10 mm) and the device is connected to a PCB circuit via contact pads and ACF cable. In the PCB circuit, probes of the DMM are connected to the respective terminals of the contact pads corresponding to



the strain gauges of the device. The DMM is connected to the laptop (LabVIEW 2015) for acquiring all the real-time data during the elongation. The device is constrained at the both ends, the entire experimental setup is shown in Fig 3.12.

There are two different strain gauges oriented in two different directions namely in direction 1 and 2 as represented in Fig 3.13. As there are two graphite strips the resistivity measurement for each graphite strip in each direction are documented individually and separately. Fig 3.14. represents the nomenclature involved to determine the strains in their respective directions. If strip1 is expanded in longitudinally, it is direction 1 and vice versa.

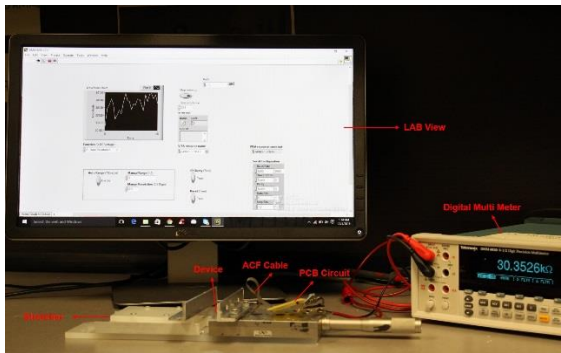


**Fig.3.13.** Experimental setup for measuring the change in the resistivity of the graphite strips due to mechanical strain

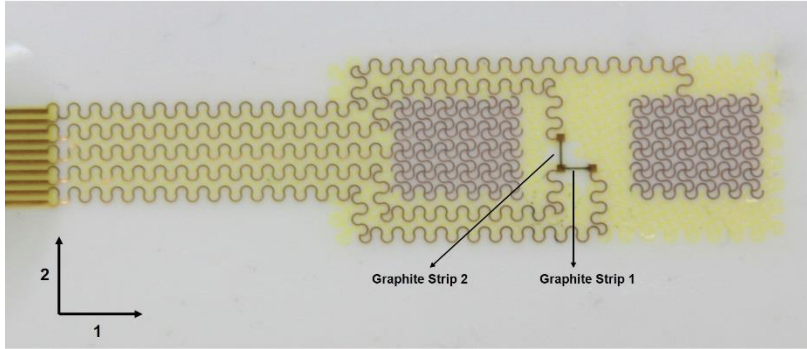


**Fig.3.14.** Nomenclature of the directions based on graphite strips

The electrodes and the strain sensor are elongated up to 20% of their original length the resulting variation in the resistivity of each graphite strip documented at every 2% of the elongation. The resistivity of the both graphite strips are measured individually. The corresponding Gauge Factor (GF) is determined by

$$GF = \Delta R / R_0 / \varepsilon \quad (13)$$

Where  $\Delta R$  is the resistance change,  $R_0$  is the initial state and  $\varepsilon$  is the strain deformation.

## 4. RESULTS

### 4.1. PEEL TEST

The force required to peel the backing layer detaching it from silicon layer spanning the length of the silicon layer is plotted as shown in Fig 4.1. The average force required to peel the backing film from silicone has been 0.038 N, as represented parameters which are evaluated to be  $b = 0.025\text{m}$  and  $\theta = 180^\circ$  (as the test conducted was 180 degree peel test) substituting these values in the Rivlin equation i.e. equation (9) gives  $3.06\text{ N/m}$  as the energy  $G_s$ .

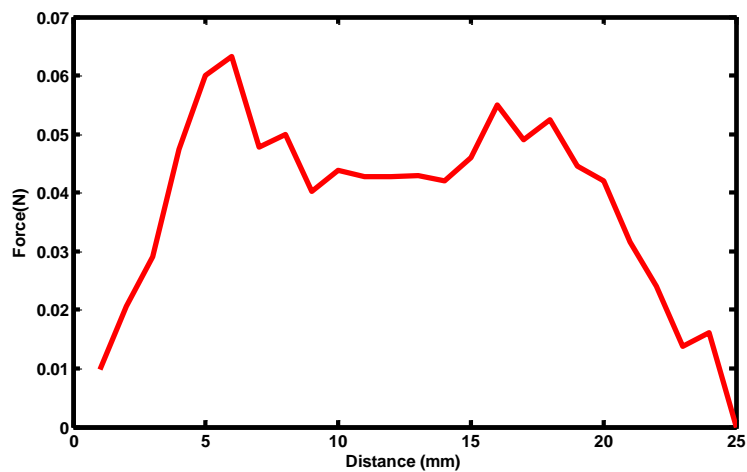


**Fig.4.1.** Force between Acetate film and Silicone

Force required to peel the adhesive layer from the silicon is plotted in Fig 4.2. Equation (8) determines the adhesive energy between silicone and the skin and the young's modulus is 350 kPa, thickness of the silicon layer is 10  $\mu\text{m}$  and substituting their respective values of those terms gives  $G_s$  as 11.95 N/m because the force required to peel was 0.058 N.

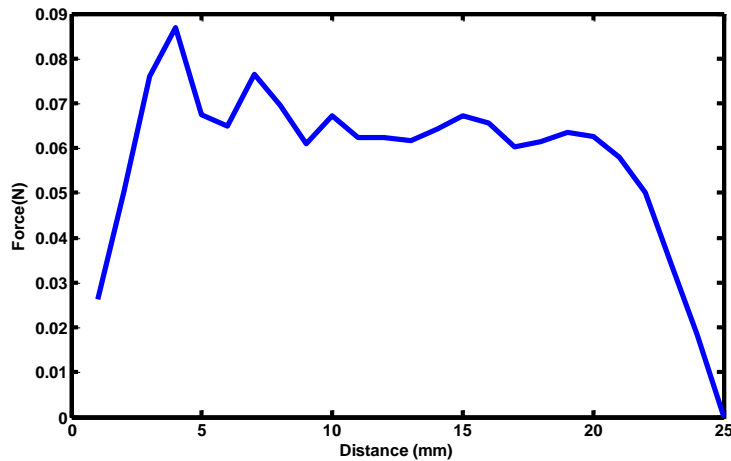


**Fig.4.2.** Force between Silicone Adhesive and Skin

From these values, the adhesive energy between the skin and the silicon adhesive is greater than adhesive energy between backing layer and silicone satisfying the condition (1).

The working energy  $G_w$  is evaluated based on the values obtained from the test with continuous peeling process. The time taken to peel the entire film was around 40 seconds

with an average of 0.041 N that gives the corresponding energy of 3.26 N/m satisfying the condition (2). Plot shown in Fig 4.3. shows the force required to peel the backing layer from the silicon layer when peeled continuously.

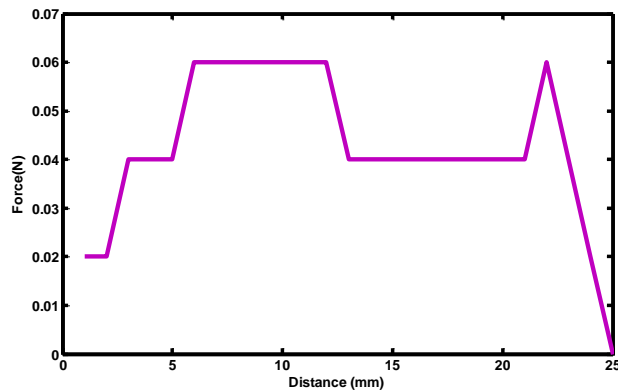


**Fig.4.3.** Force vs Time for Acetate Film and Silicone

#### **4.2. RESPONSE OF THE EP SENSORS FROM THE IN-VIVO TEST**

The device is placed on various locations of the human body for measuring the physiological signals. The position of the device over the body determines the kind of physiological signal as mentioned in the earlier sections. The backing layer should be peeled out after placing the device and the measurement can be commenced. EEG signals are obtained by mounting the sensor over the scalp as shown in Fig 4.4. And the corresponding filtered signal is shown Fig 4.5.

The placement of the device for the EOG signals is shown in the Fig 4.6. The filtered EOG signal can be analyzed as per the eye blink movement there is an increase in the signal crests and troughs for every blink. Each such part of the signal represents one eye blink as shown in Fig 4.7.



**Fig.4.4.** Sensor location on the scalp for EEG measurement

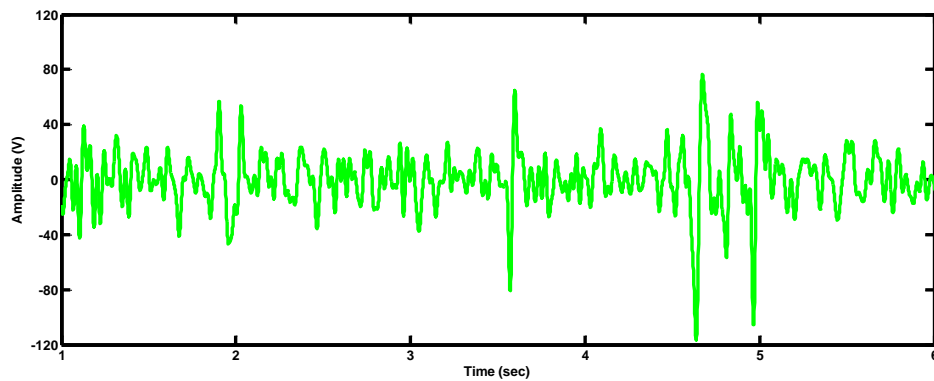


**Fig.4.5.** Plot of EEG signals obtained as per the position shown in Fig 4.4.

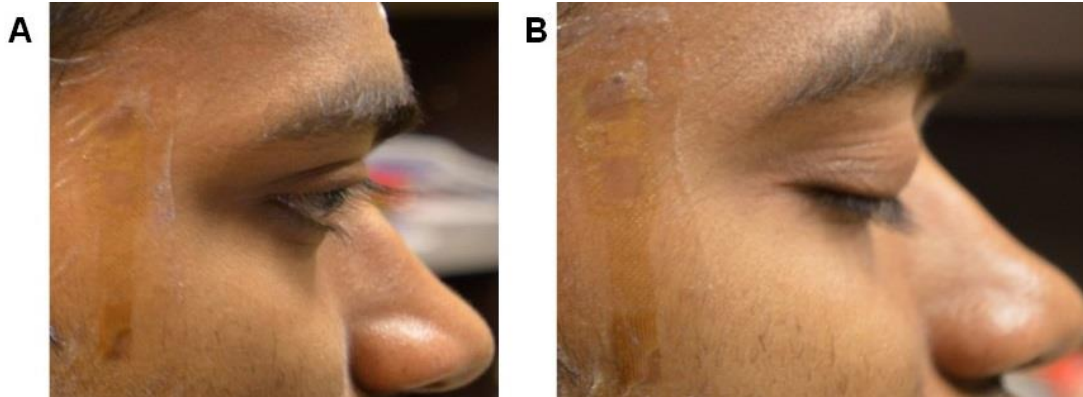


**Fig.4.6.** Sensor location on the scalp for EOG measurement

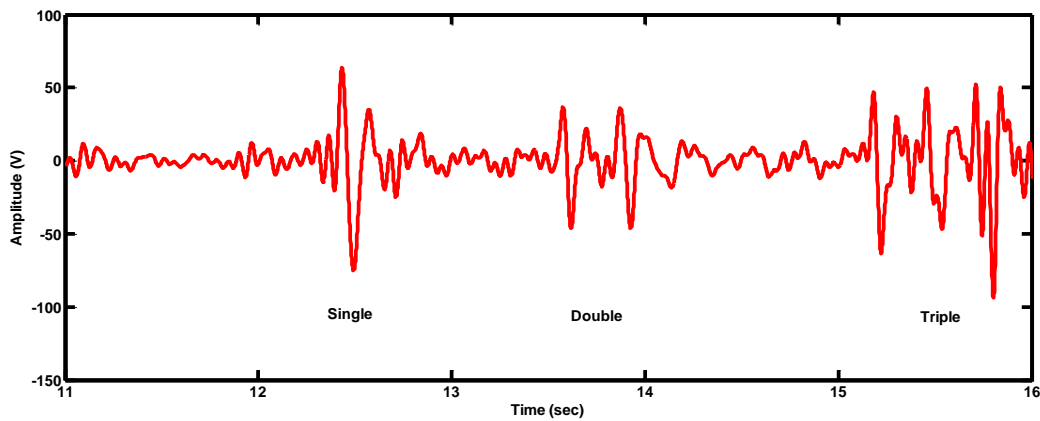


**Fig.4.7.** Plot of EOG signals obtained as per the position shown in Fig. 4.6.

The capturing of surface EMG signals can be illustrated with a jaw activity. The position of the device for obtaining the corresponding physiological signals from the cheek activity as shown in the Fig 4.8. The obtained EMG signal during random opening and closing of the cheek signifies the jaw activity; the filtered signal as shown in Fig 4.9. The

abnormality in the signal signifies the movement in the jaw. Graph in Fig 4.9 shows signal activity due to single double and triple opening of the jaw.

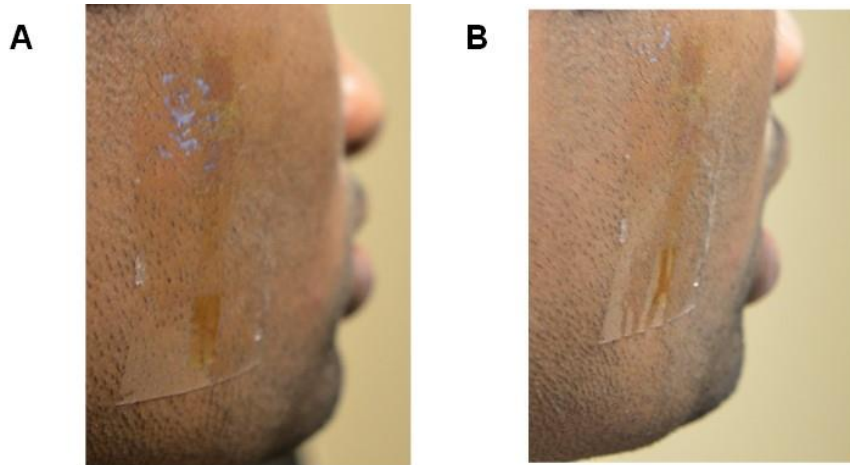


**Fig.4.8.** Sensor location on the scalp for EMG measurement

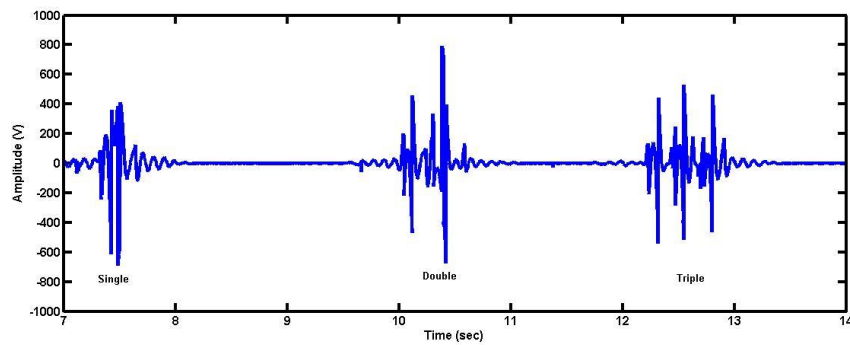


**Fig.4.9.** Plot of EOG signals obtained as per the position shown in Fig 4.8.



### 4.3. RESPONSE OF THE STRAIN SENSORS FROM THE IN-VITRO TEST

The Graphite layers record mechanical movements and play vital role as kinematic sensors. The percentage change in resistance of the graphite strips when graphite strips are expanded mechanically. Figs 4.10 & 4.11 are the plots obtained when the graphite strips are elongated in direction1 and direction 2 respectively.

The gauge factor for the graphite strips in direction1 and direction2 are calculated as per the equation (13) and tabulated in Table 4.1.

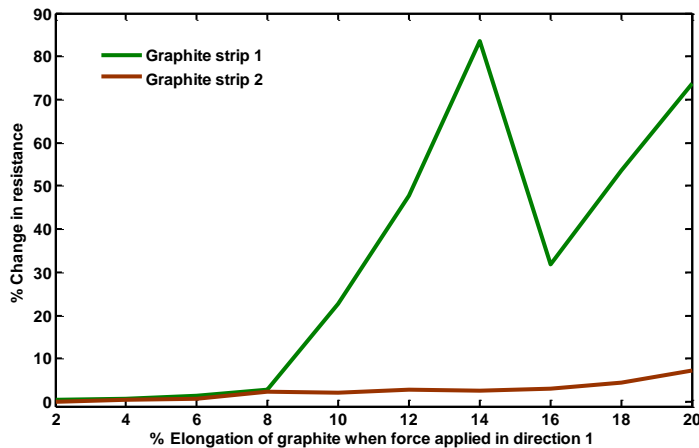


**Fig.4.10.** Percentage Change in resistance of the graphite strips when expanded in direction 1

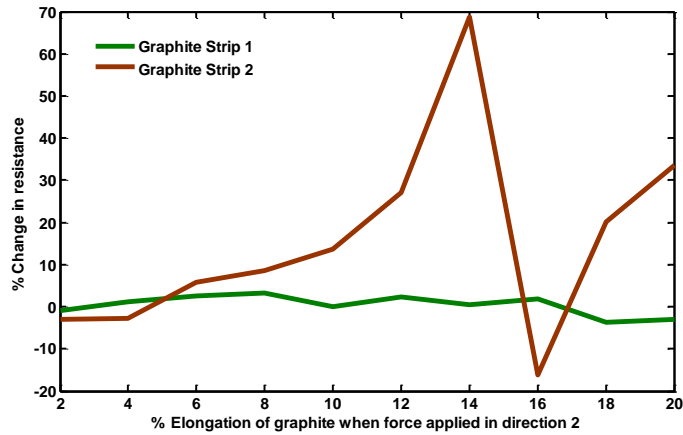


**Fig.4.11.** Percentage Change in resistance of the graphite strips when expanded in direction 2

**Table.4.1.** Gauge factor of the graphite strips in direction1 & 2

	Direction 1	Direction 2
Graphite Strip 1	3.665	0.3665
Graphite Strip 2	0.1534	1.6756

## 5. SUMMARY AND CONCLUSIONS

In summary, the work reported here illustrates advantages in EP measurements that follow from the concepts of epidermal electronics. The resulting devices offer enhanced levels of wearability, expanded options in device sterilization and minimized artifacts from body motions compared to previously reported technologies, including direct contact epidermal electrodes.

Modifications in the external Bluetooth circuit can increase the capability to measure different kinds of physiological measurements from the device. Strain gauge using graphite ink instead of graphite powder might enhance the gauge factor and even sensitive to change in temperature. In case of using the epidermal device for a long-term physiological measurement, the silicon membrane can be perforated using a 3d perforator array in order to avoid the accumulation of sweat. The silicone adhesive may lose its property to stick with the increase of bio-fluids between the silicon membrane and the skin.

Exploring these options, integrating signal processing, and wireless data transmission capabilities into the EES represents promising directions for future research. Such technology would build on advances in telemedicine and ubiquitous healthcare.

## **6. ACKNOWLEDGEMENT**

Missouri University of Science & Technology and National Science Foundation (NSF) supported the research reported in the paper. The authors gratefully acknowledge their support. Any findings or conclusions are to the authors and do not reflect the sponsors.

## REFERENCES

- [1] Šušmáková, Kristina. "Human sleep and sleep EEG." *Measurement science review* 4.2 (2004): 59-74.
- [2] Institute of Medicine (US) Committee on Sleep Medicine and Research; Colten HR, Altevogt BM, editors. *Sleep Disorders and Sleep Deprivation: An Unmet Public Health Problem*. Washington (DC): National Academies Press (US); 2006. 2, Sleep Physiology.
- [3] Heide, W., et al. "Electrooculography: technical standards and applications." *Electroencephalogr Clin Neurophysiol* 1999 (1999): 223-40.
- [4] Jacobs L, Feldman M, Bender MB. Eye Movements during Sleep: I. the Pattern in the Normal Human. *Arch Neurol*.1971; 25(2):151-159. doi:10.1001/archneur.1971.00490020069008.
- [5] Geyer, James D., Sachin Talathi, and Paul R. Carney. "Introduction to sleep and polysomnography." *Reading EEGs: a practical approach*, Lippincott Williams & Wilkins, Philadelphia (2009).
- [6] Jaakko Malmivuo & Robert Plonsey: *Bioelectromagnetism - Principles and Applications of Bioelectric and Biomagnetic Fields*, Oxford University Press, New York, 1995. Chapter 13.
- [7] American Association of Sleep Technologists *sleep technology: Technical Guideline Standard Polysomnography*, 2510 North Frontage Road, Darien, IL, 2012.
- [8] Tsuno, Norifumi, Alain Besset, and Karen Ritchie. "Sleep and depression." *Journal of Clinical Psychiatry* (2005).
- [9] Hiestand, David M., et al. "Prevalence of symptoms and risk of sleep apnea in the US population: Results from the national sleep foundation sleep in America 2005 poll." *CHEST Journal* 130.3 (2006): 780-786.
- [10]. Chung, Ka-Fai, et al. "Cross-cultural and comparative epidemiology of insomnia: the Diagnostic and Statistical Manual (DSM), International Classification of Diseases (ICD) and International Classification of Sleep Disorders (ICSD)." *Sleep medicine* 16.4 (2015): 477-482.
- [11]. Ram, Saravanan, et al. "Prevalence and impact of sleep disorders and sleep habits in the United States." *Sleep and breathing* 14.1 (2010): 63-70.

[12]. Kushida, Clete A., et al. "Practice parameters for the indications for polysomnography and related procedures: an update for 2005." *Sleep* 28.4 (2005): 499-521.

[13]. Foley, Daniel, et al. "Sleep disturbances and chronic disease in older adults: results of the 2003 National Sleep Foundation Sleep in America Survey." *Journal of psychosomatic research* 56.5 (2004): 497-502.

[14]. Chesson, A. L., et al. "Practice parameters for the indications for polysomnography and related procedures." *Sleep* 20.6 (1997): 406-422.

[15]. Mellinger, Glen D., Mitchell B. Balter, and Eberhard H. Uhlenhuth. "Insomnia and its treatment: prevalence and correlates." *Archives of general psychiatry* 42.3 (1985): 225-232.

[16]. Kushida, Clete A., et al. "Practice parameters for the indications for polysomnography and related procedures: an update for 2005." *Sleep* 28.4 (2005): 499-521.

[17] Gresham, S. C., H. W. Agnew, and Robert L. Williams. "The sleep of depressed patients: An EEG and eye movement study." *Archives of General Psychiatry* 13.6 (1965): 503-507.

[18] Oswald, Ian. "Falling asleep open-eyed during intense rhythmic stimulation." *British medical journal* 1.5184 (1960): 1450.

[19] João Cordovil Bárcia-Human electrooculography interface, Instituto superior Tecnico Universidade Technical de Lisboa, Lisboa, October 2010.

[20] José Guerreiro- A Bio signal Embedded System for Physiological Computing, INSTITUTO SUPERIOR DE ENGENHARIA DE LISBOA, October 2013.

[21] Alshaer, Hisham, et al. "Comparison of in-laboratory and home diagnosis of sleep apnea using a cordless portable acoustic device." *Sleep Medicine*.

[22] Bar, Amir, et al. "Evaluation of a portable device based on peripheral arterial tone for unattended home sleep studies." *CHEST Journal* 123.3 (2003): 695-703.

[23] Ng, Susanna SS, et al. "Validation of Embletta portable diagnostic system for identifying patients with suspected obstructive sleep apnoea syndrome (OSAS)." *Respirology* 15.2 (2010): 336-342.

[24] Ng, S. S. S., et al. "Validation of a portable recording device (ApneaLink) for identifying patients with suspected obstructive sleep apnoea syndrome." *Internal medicine journal* 39.11 (2009): 757-762.

- [25] Patel, Minal R., Thomas H. Alexander, and Terence M. Davidson. "Home sleep testing." *Operative Techniques in Otolaryngology-Head and Neck Surgery* 18.1 (2007): 33-51.
- [26] Grover, Sukhdev S., and Stephen D. Pittman. "Automated detection of sleep disordered breathing using a nasal pressure monitoring device." *Sleep and Breathing* 12.4 (2008): 339-345.
- [27] Hung, K., Y. T. Zhang, and B. Tai. "Wearable medical devices for tele-home healthcare." *Engineering in Medicine and Biology Society, 2004. IEMBS'04. 26th Annual International Conference of the IEEE. Vol. 2. IEEE, 2004.*
- [28] de Zambotti, Massimiliano, et al. "Evaluation of a consumer fitness-tracking device to assess sleep in adults." *Chronobiology international* 32.7 (2015): 1024-1028.
- [29] Dick, R., et al. "AASM standards of practice compliant validation of actigraphic sleep analysis from SOMNOWatch™ versus polysomnographic sleep diagnostics shows high conformity also among subjects with sleep disordered breathing." *Physiological measurement* 31.12 (2010): 1623.
- [30] Bulling, Andreas, Daniel Roggen, and Gerhard Tröster. *Wearable EOG goggles: eye-based interaction in everyday environments.* ACM, 2009.
- [31] Manabe, Hiroyuki, and Masaaki Fukumoto. "Full-time wearable headphone-type gaze detector." *CHI'06 Extended Abstracts on Human Factors in Computing Systems.* ACM, 2006.
- [32] Costanza, Enrico, et al. "Intimate interfaces in action: Assessing the usability and subtlety of EMG-based motionless gestures." *Proceedings of the SIGCHI conference on Human factors in computing systems.* ACM, 2007.
- [33] Moon, Inhyuk, et al. "Wearable EMG-based HCI for electric-powered wheelchair users with motor disabilities." *Robotics and Automation, 2005. ICRA 2005. Proceedings of the 2005 IEEE International Conference on.* IEEE, 2005.
- [34] Kim, Dae-Hyeong, et al. "Epidermal electronics." *science* 333.6044 (2011): 838-843.
- [35] Jeong, Jae-Woong, et al. "Materials and Optimized Designs for Human-Machine Interfaces Via Epidermal Electronics." *Advanced Materials* 25.47 (2013): 6839-6846.
- [36] Yeo, Woon-Hong, et al. "Multifunctional epidermal electronics printed directly onto the skin." *Advanced Materials* 25.20 (2013): 2773-2778.

[37] Jeong, Jae-Woong, et al. "Capacitive Epidermal Electronics for Electrically Safe, Long-Term Electrophysiological Measurements." *Advanced healthcare materials* 3.5 (2014): 642-648. (ECG,EOG, EMG).

[38] Kim, Jeonghyun, et al. "Epidermal Electronics with Advanced Capabilities in Near-Field Communication." *Small* 11.8 (2015): 906-912.

[39] Amjadi, Morteza, et al. "Highly stretchable and sensitive strain sensor based on silver nanowire–elastomer nanocomposite." *ACS nano* 8.5 (2014): 5154-5163.

[40] Wang, Shuodao, et al. "Mechanics of epidermal electronics." *Journal of Applied Mechanics* 79.3 (2012): 031022.

[41] Xu, Sheng, et al. "Soft microfluidic assemblies of sensors, circuits, and radios for the skin." *Science* 344.6179 (2014): 70-74.

[42] Huang, Xian, et al. "Materials and designs for wireless epidermal sensors of hydration and strain." *Advanced Functional Materials* 24.25 (2014): 3846-3854.

[43] Huang, Xian, et al. "Epidermal impedance sensing sheets for precision hydration assessment and spatial mapping." *Biomedical Engineering, IEEE Transactions on* 60.10 (2013): 2848-2857.

[44] Huang, Xian, et al. "Stretchable, wireless sensors and functional substrates for epidermal characterization of sweat." *small* 10.15 (2014): 3083-3090.

[45] Gao, Li, et al. "Epidermal photonic devices for quantitative imaging of temperature and thermal transport characteristics of the skin." *Nature communications* 5 (2014).

[46] Kendall, K. "Thin-film peeling—the elastic term." *Journal of Physics D: Applied Physics* 8.13 (1975): 1449.

[47] Kovalchick, Christopher, and Alain Molinari. "MECHANICS OF PEELING FOR EXTENSIBLE ELASTIC ADHESIVE TAPES." (2009).

[48] Yarusso, D. J. "Adhesion Science and Engineering—The Mechanics of Adhesion, edited by DA Dillard and AV Pocius." (2002): 499-534.

[49] Carlo J. De Luca, L. Donald Gilmore, Mikhail Kuznetsov, Serge H. Roy, Filtering the surface EMG signal: Movement artifact and baseline noise contamination, *Journal of Biomechanics*, Volume 43, Issue 8, 28 May 2010, Pages 1573-1579, ISSN 0021-9290.



[50] E. Huigen, A. Peper, C.A. Grimbergen, Investigation into the origin of the noise of surface electrodes, *Medical and Biological Engineering and Computing*, 40 (2002), pp. 332–338.

[51] Stegeman D.F. and Hermens H.J., 1998. Standards for surface electromyography: the European project (SENIAM). In: Hermens H.J., Rau G., Disselhorst-Klug C., Freriks B. (Eds.), *Surface Electromyography Application Areas and Parameters. Proceedings of the Third General SENIAM Workshop on surface electromyography*, Aachen, Germany, pp. 108–112.

[52] A. van Boxtel, A.J.W. Boelhouwer, A.R. Bos, Optimal EMG signal bandwidth and interelectrode distance for the recording of acoustic, electro cutaneous, and photic blink reflexes, *Psychophysiology*, 35 (1998), pp. 690–697.

[53] Fatourechi, Mehrdad, et al. "EMG and EOG artifacts in brain computer interface systems: A survey." *Clinical neurophysiology* 118.3 (2007): 480-494.

[54] American Association of Sleep Technologists sleep technology: Technical Guideline Standard Polysomnography, 2510 North Frontage Road, Darien, IL, 2012.

## VITA

J V M S Avinash Kankipati was born in Vijayawada, India. He received his Bachelor of Engineering (B.E) in Mechanical Engineering from K.L.Univeristy, Vaddeswaram, India in 2013. He has been pursuing his graduate studies in the Department of Mechanical and Aerospace Engineering at Missouri University of Science and Technology (formerly University of Missouri - Rolla) since January 2013. During his stay at Missouri University of Science and Technology, he held the position of Graduate Research Assistant. He received his Master of Science degree in Mechanical Engineering from Missouri University of Science and Technology, Rolla, Missouri, USA, in May 2016.